AMEGHINIANA
A GONDWANAN PALEONTOLOGICAL JOURNAL

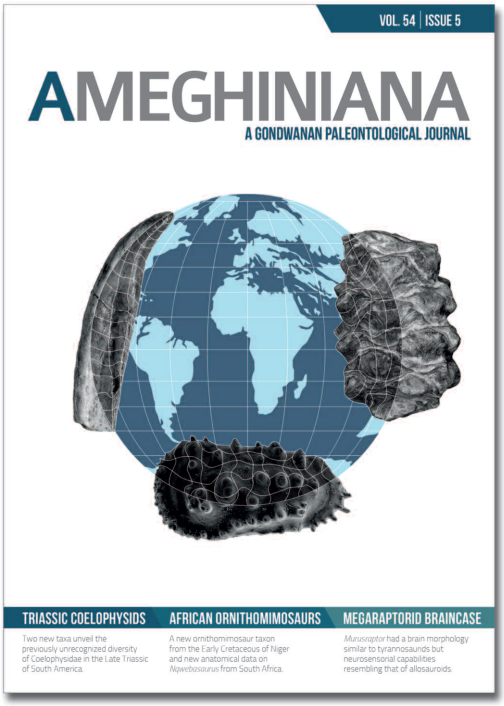

EARLY CRETACEOUS ORNITHOMIMOSAURS (DINOSAURIA: COELUROSAURIA) FROM AFRICA

PAUL C. SERENO

Department of Organismal Biology and Anatomy and Committee on Evolutionary Biology, University of Chicago, 1027 East 57th Street, Chicago, Illinois, 60637, U.S.A.

Submitted: August 5th, 2017 - **Accepted:** October 23rd, 2017 - **Published online:** November 1st, 2017

To cite this article: Paul C. Sereno (2017). Early Cretaceous ornithomimosaurs (Dinosauria: Coelurosauria) from Africa. *Ameghiniana* 54: 576–616.

To link to this article: http://dx.doi.org/10.5710/AMGH.23.10.2017.3155

ISSN 0002-7014
GONDWANAN PERSPECTIVES AMEGHINIANA - 2017 - Volume 54 (5): 576 – 616

EARLY CRETACEOUS ORNITHOMIMOSAURS (DINOSAURIA: COELUROSAURIA) FROM AFRICA

PAUL C. SERENO

Department of Organismal Biology and Anatomy and Committee on Evolutionary Biology, University of Chicago, 1027 East 57th Street, Chicago, Illinois, 60637, U.S.A.
dinosaur@uchicago.edu

Abstract. A new genus and species of ornithomimosaur, *Afromimus tenerensis*, is described based on a fragmentary skeleton from the Lower Cretaceous (Aptian–Albian) El Rhaz Formation of Niger. The holotype and only known individual preserves caudal vertebrae, chevrons and portions of the right hind limb. Derived ornithomimosaurian features include the broad, peanut-shaped articular surfaces of mid caudal centra, parasagittal fossae on mid caudal centra for reception of the postzygapophyses of the preceding vertebra, and a raised, subtriangular platform on the ventral aspect of the pedal phalanges. New information is given for, and comparisons made to, *Nqwebasaurus thwazi* from southern Africa, the oldest and most basal ornithomimosaur. Unlike other coelurosaurian clades that have expansive radiations on northern landmasses, the oldest ornithomimosaur and now another basal form are known from a southern landmass, Africa.

Key words. Theropoda. Ornithomimosauria. Ornithomimid. Paleobiogeography. Gondwana. *Afromimus. Nqwebasaurus.*

Resumen. ORNITHOMIMOSAURIOS DEL CRETÁCICO TEMPRANO (DINOSAURIA: COELUROSAURIA) DE ÁFRICA. Un nuevo género y especie de ornithomimosaurio, *Afromimus tenerensis*, es descrito en base a un esqueleto fragmentario de la Formación El Rhaz del Cretácico Temprano (Aptiano–Albiano) de Nigeria. El holotipo y único individuo conocido preserva vértebras caudales, chevrones, y portiones del miembro posterior derecho. Las características derivadas de ornithomimosaurios incluyen superficie articular de caudales medias en forma de maní, fosas parasagitales en centros de caudales medias para la recepción de postzygapófisis de la vértebra precedente, y una plataforma subtriangular elevada en la cara ventral de la falanges. La nueva información se da, y se compara con, *Nqwebasaurus thwazi* del sur de África, el ornitomimosaurio más antiguo y más basal. En contraposición a otros clados coelurosauriios que poseen una radiación expansiva en las masas continentales del hemisferio norte, el ornitomimosaurio más antiguo y ahora otra forma basal provienen de una masa continental del sur, África.

Palabras clave. Theropoda. Ornithomimosauria. Ornitomímido. Oaleobiogeografía. Gondwana. *Afromimus. Nqwebasaurus.*

Ornithomimosaurs are best known from Late Cretaceous deposits on northern landmasses. These well known genera include *Gallimimus* (Osmólska *et al.*, 1972), *Garudimimus* (Barsbold, 1981; Kobayashi and Barsbold, 2005a), *Deinocheirus* (Osmólska and Roniewicz, 1970; Lee *et al.*, 2014), and *Sinornithomimus* (Kobayashi and Lü, 2003) from Asia and *Ornithomimus* (Sternberg, 1933) and *Struthiomimus* (Osborn, 1917) from Laramidia. Similarly, older ornithomimosaurs of late Early Cretaceous age (Berriasian to Aptian) also are found only on northern landmassses. The most complete of these include *Harpymimus* (Barsbold and Perle, 1984; Kobayashi and Barsbold, 2005b) and *Shenzhosaurus* (Ji *et al.*, 2003) from Asia, and *Pelecanimimus* (Perz-Moreno *et al.,* 1994) and the Angeac ornithomimosaur (Allain *et al.*, 2014) from western Europe.

Other fragmentary Early Cretaceous ornithomimosaurs from Laurasian rocks include *Valdoraptor* and other isolated postcrania from Valanginian-to-Berriasian-age rocks in southern England (Allain *et al.*, 2014), *Nedcolbertia* from Berriasian-age rocks in Utah (Kirkland *et al.*, 1998; Brownstein, 2017), and *Kinnareemimus* from ?Berriasian-age rocks in Thailand (Buffetaut *et al.*, 2009). Together, these widespread, fragmentary materials suggest that Early Cretaceous strata on Laurasia will eventually reveal important early stages in the evolution of Ornithomimosauria.

Other taxa from Laurasian landmasses have been described recently as ornithomimosaurs, although their morphology and affinity remain poorly established. These include *Hexing* from ?Berriasian rocks in northern China (Jin *et al.*, 2012) and *Lepidocheirosaurus* from Late Jurassic (?Tithonian) rocks in Transbaikal Siberia (Alifanov and Saveliev, 2015). The partial holotypic skeleton of *Hexing* is very poorly preserved with some portions of the skeleton, such as the manus, exhibiting morphology and phalangeal

 AMGHB2-0002-7014/12$00.00+.50

formula unlike that of any ornithomimosaur. These same deposits, it should be noted, yielded the well-preserved ornithomimosaur *Shenzhousaurus* (Ji *et al*., 2003). The remains of *Lepidocheirosaurus* are extremely fragmentary, the holotype limited to portions of the left manus and referred material to a few isolated caudal vertebrae. Its identification as an ornithomimosaur and the diagnosis of the species are not based on synapomorphies and autapomorphies, respectively, and so the affinity and basis for this taxon remain problematic.

Southern "ornithomimosaurs" reassigned. Initial reports of ornithomimosaurs from southern landmasses have been reassigned to other theropod clades or questioned as ornithomimosaurs. The Late Jurassic *Elaphosaurus bambergi* from Tanzania, formerly interpreted as an ornithomimosaur (Galton, 1982), has been reevaluated as an abelisauroid (noasaurid) theropod (Holtz, 1994; Rauhut and Caranno, 2016). The Early Cretaceous (Aptian–Albian) *Timimus hermani* from the southern coast of Australia (Rich and Rich, 1994) was based on isolated femora more likely referable to Dromaeosauridae (Agnolin *et al*., 2010).

Nqwebasaurus*, southern basal ornithomimosaur.* The southern African genus *Nqwebasaurus* (de Klerk *et al*., 2000; Choiniere *et al*., 2012) is known from a single partial skeleton discovered in Early Cretaceous (Berriasian–Valanginian) rocks of southern Africa. *Nqwebasaurus*, first recognized as an ornithomimosaur by Sereno (2001), stands as the only accepted representative of this clade from a southern landmass—and the oldest ornithomimosaur on record.

A new southern ornithomimosaur. Here I describe a second ornithomimosaur from Africa of slightly younger age than *Nqwebasaurus*. The holotypic and only known specimen was discovered in 1997 in the Ténéré Desert (Gadoufaoua) of Niger in the Lower Cretaceous (Aptian–Albian) El Rhaz Formation. Further details, in addition, are given for *Nqwebasaurus* to supplement previous descriptions (de Klerk *et al*., 2000; Choiniere *et al*., 2012). These southern ornithomimosaurs may point to an early phase in the evolution of the clade prior to its diversification on northern landmasses in the late Early and Late Cretaceous (Allain *et al*., 2014).

MATERIALS AND METHODS

Anatomical orientation and taxonomic terminology. Common directional terms (*e.g*., "anterior") and Romerian anatomical terms are used here as opposed to veterinarian directional (*e.g*., "rostral") and anatomical (*e.g*., "alular digit") terms used within the crown group Aves (see Wilson, 2006). Regarding taxonomic terminology, Ornithomimosauria and Ornithomimidae, are used as defined by Sereno (2005a,b), the former a stem-based taxon including *Nqwebasaurus thwazi* and all species closer to *Ornithomimus edmontonicus* than a range of other coelurosaurian clades (Tab. 2). Ornithomimidae is also a stem-based taxon circumscribing the best known Late Cretaceous species, while excluding the more basal Early Cretaceous species *Shenzhousaurus orientalis, Harpymimus okladnikovi, Pelecanimimis polyodon*, and *Garudimimus brevipes* (Tab. 2).

Ornithomimoidea Marsh 1890, following traditional use of suffixes in Linnean taxonomy, should circumscribe a clade more inclusive than Ornithomimidae but less inclusive than Ornithomimosauria, a suprafamilial taxon. As is apparent below, *Nqwebasaurus thwazi* is decisively more primitive in many skeletal features than other species of Early Cretaceous age (*e.g*., *Shenzhousaurus oreintalis*, *Harpymimus okladnikovi* and *Pelecanimimis polyodon*). The taxon Ornithomimoidea, thus, could be a heuristic stem-based clade to encompass all ornithomimosaurs more advanced than *Nqwebasaurus thwazi*. To that end, a definitional revision is proposed here for Ornithomimoidea Marsh 1890 (Tab. 2), a taxon initially defined by Sereno (1999a, 1999b) to encompass ornithomimids and alvarezsaurids, prior to the discovery of basal taxa within each subgroup that have undermined their monophyly).

Fossil preservation. The holotype and only known specimen of *Afromimus tenerensis* (MNBH GAD112; Figs. 1–10) was weathering on a nearly horizontal erosional surface and may have been considerably more complete when originally buried. No other vertebrate fossils were preserved at the type locality, and no other specimens pertaining to an ornithomimosaur have been reported from other localities in the El Rhaz Formation.

Caudal vertebrae, chevrons, and a rib shaft fragment were found out of place although near the crus. One vertebra, the distalmost caudal vertebra (CA ?27), was found a few meters away. The seven preserved caudal vertebrae can be arranged in a morphological series (with gaps) that span the middle portion of the tail (Figs. 1, 2; Tab. 1). Both preserved chevrons are from the proximal one half of the

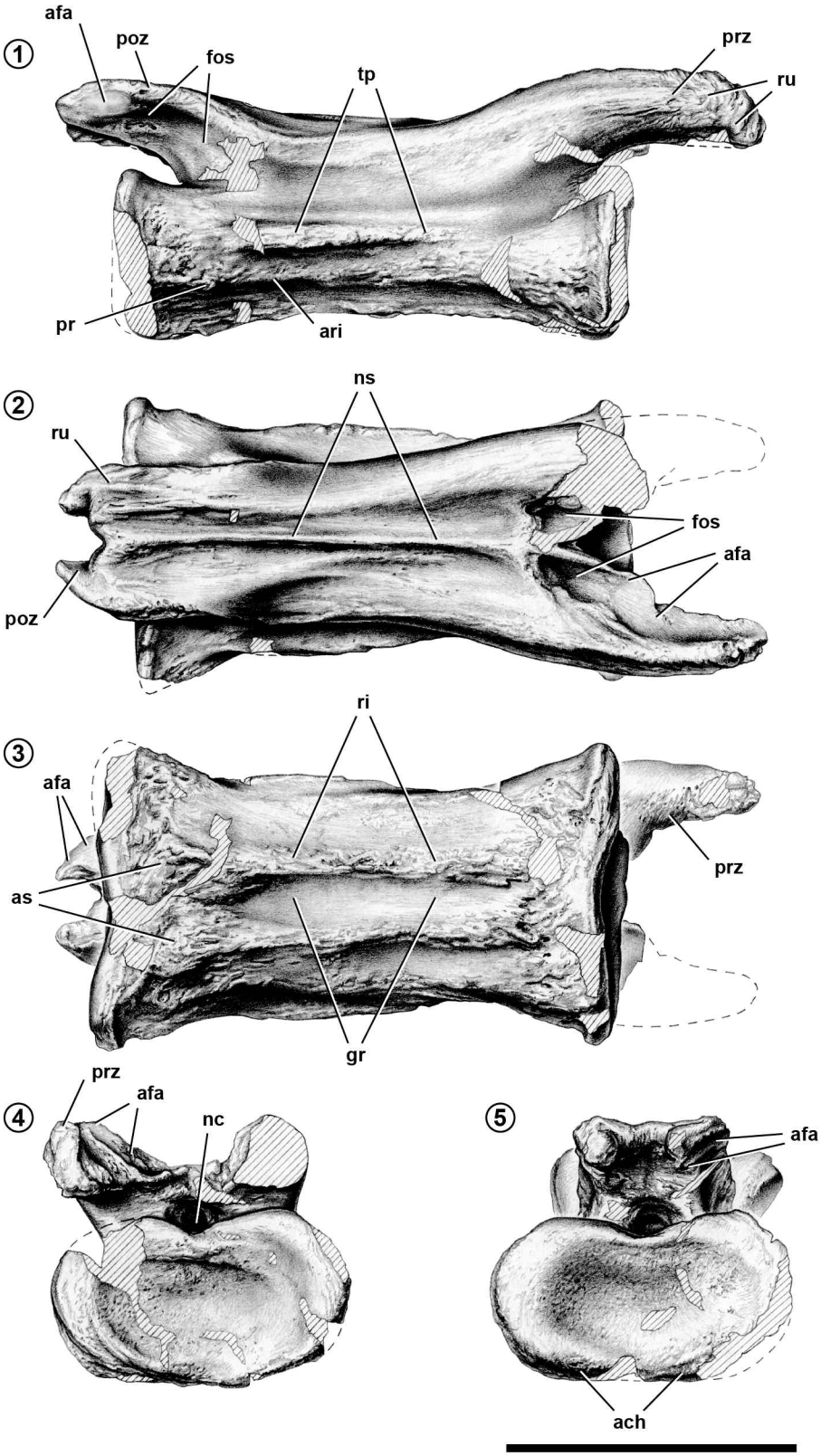

Figure 1. 1–5, ***Afromimus tenerensis*** gen. et sp. nov., **MNBH GAD**112. Drawings of caudal vertebra ?16 in **1,** right lateral view; **2,** dorsal view; **3,** ventral view; **4,** anterior view; **5,** posterior view. Hatching indicates a broken surface; dashed line indicates a missing margin. Abbreviations: **ach,** articular surface for chevron; **afa,** articular facet; **ari**, accesory ridge; **as,** attachment surface; **fos,** fossa; **gr,** groove; **nc,** neural canal; **ns,** neural spine; **poz,** postzygapohpysis; **pr**, process; **prz,** prezygapohysis; **ri,** ridge; **ru,** rugosity; **tp,** transverse process. Scale bar= 3 cm.

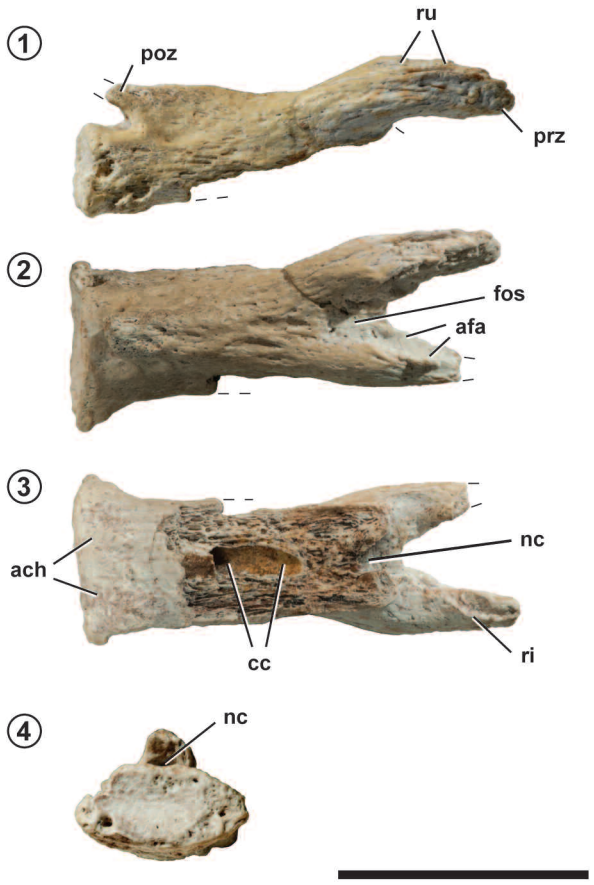

Figure 2. 1–4, *Afromimus tenerensis* gen. et sp. nov., **MNBH GAD**112. Caudal vertebra ?24 in **1,** left lateral view; **2,** dorsal view; **3**, ventral view; **4**, posterior view. Dashed line indicates a missing margin. Abbreviations: **ach,** articular surface for chevron; **afa,** articular facet; **cc**, central cavity; **fos,** fossa; **nc,** neural canal; **poz,** postzygapohpysis; **prz,** prezygapohysis; **ri,** ridge; **ru,** rugosity. Scale bar= 3 cm.

tail (Fig. 3) based on comparisons to other ornithomimosaurs (Kobayashi and Barsbold, 2005).

The right tibia, fibula and portions of the coossified proximal tarsals were discovered *in situ*, although considerably weathered (Figs. 4–8). Portions of three pedal phalanges are preserved (Figs. 9, 10; Tab. 3). If they pertain to the right hind limb as does the preserved crus, they appear to represent the distal end of pedal phalanx II-2 and ungual of pedal digit II (Figs. 9.3–9.5, 10) and the proximal end of pedal phalanx III-1 (Fig. 9.1, 9.2).

Fossil preparation. The holotypic specimen of *Afromimus tenerensis* (MNBH GAD112) was prepared mechanically with airscribe and pin vise. The distal end of the fibula is partially coossified to the astragalus and calcaneum, although not to the underlying tibia (Fig. 8). As a result, the coossified fibula-distal tarsal piece could be lifted away from the end of the tibia with only a small fragment of the calcaneum adhering to the tibial flange (Fig. 6.1).

Skeletal maturity and adult body size. The holotypic specimen of *Afromimus tenerensis* (MNBH GAD112) most likely had reached adult body size, given the complete fusion of all neurocentral sutures in the caudal vertebrae and partial fusion of the crus to the proximal tarsals. At just over 40 cm, the tibia is comparable in length to the largest specimen of the early Late Cretaceous ornithomimid *Sinornithomimus dongi* (LH PV7) recovered from a mud-trapped herd site in Inner Mongolia (Varricchio *et al.*, 2008). That specimen, however, is a subadult with a minimum age of seven years. Thus the new African ornithomimoid would have had a somewhat smaller adult body size than *Sinornithomimus dongi* and approxiamtely one half that of the largest specimens of the Late Cretaceous *Gallimumus bullatus* (Osmólska *et al.*, 1972). The size of the new ornithomimosaur, nonetheless, is approximately twice that of the Early Cretaceous ornithomimosaur, *Shenzhousaurus dongi* (Ji *et al.*, 2003), and three times that of *Nqwebasaurus thwazi* (de Klerk *et al.*, 2000).

Institutional abbreviations. **AM,** Albany Museum, Grahamstown, South Africa; **IVPP,** Institute of Vertebrate Paleontology and Paleoanthropology, Beijing, China; **LH,** Long Hao Institute for Stratigraphic Paleontology, Inner Mongolia, China; **LHo,** Museo de Cuenca, Cuenca, Spain; **MNBH,** Musée national Boubou Hama, Niamey, République du Niger; **TMP,** Royal Tyrrell Museum of Palaeontology, Drumheller, Canada.

SYSTEMATIC PALEONTOLOGY

Dinosauria Owen, 1842
Saurischia Seeley, 1888
Theropoda Marsh, 1891
Coelurosauria Huene, 1914
Ornithomimosauria Barsbold, 1976

Afromimus gen. nov.
Figures 1–10

Type species. *Afromimus tenerensis*.
Etymology. *Afro*-(L.), Africa; *mimos* (Gr.), mimic.
Diagnosis. Same as for type species.

Afromimus tenerensis sp. nov.

Etymology. *tenere-* (Fr.) Ténéré Desert; *-ensis* (L.), from.

Holotype. Fragmentary remains of an adult individual comprising a dorsal rib fragment, seven partial mid and distal caudal vertebrae, two partial chevrons, most of the right tibia and fibula, coossified proximal tarsals, and three partial pedal phalanges including a pedal ungual (MNBH GAD112).

Type locality. 16° 22′ N, 9° 1′ E, Gadoufaoua, Ténéré Desert, Niger Republic. The tibia, fibula, astragalus and calcaneum were articulated and found *in situ*. All other bones except the distalmost preserved caudal vertebra were scattered nearby within a radius of one meter. No other fossil vertebrates were found *in situ* in the vicinity of the specimen.

Formation and age. El Rhaz Formation, Early Cretaceous (Aptian–Albian).

Diagnosis. Medium-sized ornithomimosaur with a large elliptical attachment scar on the posterior aspect of the

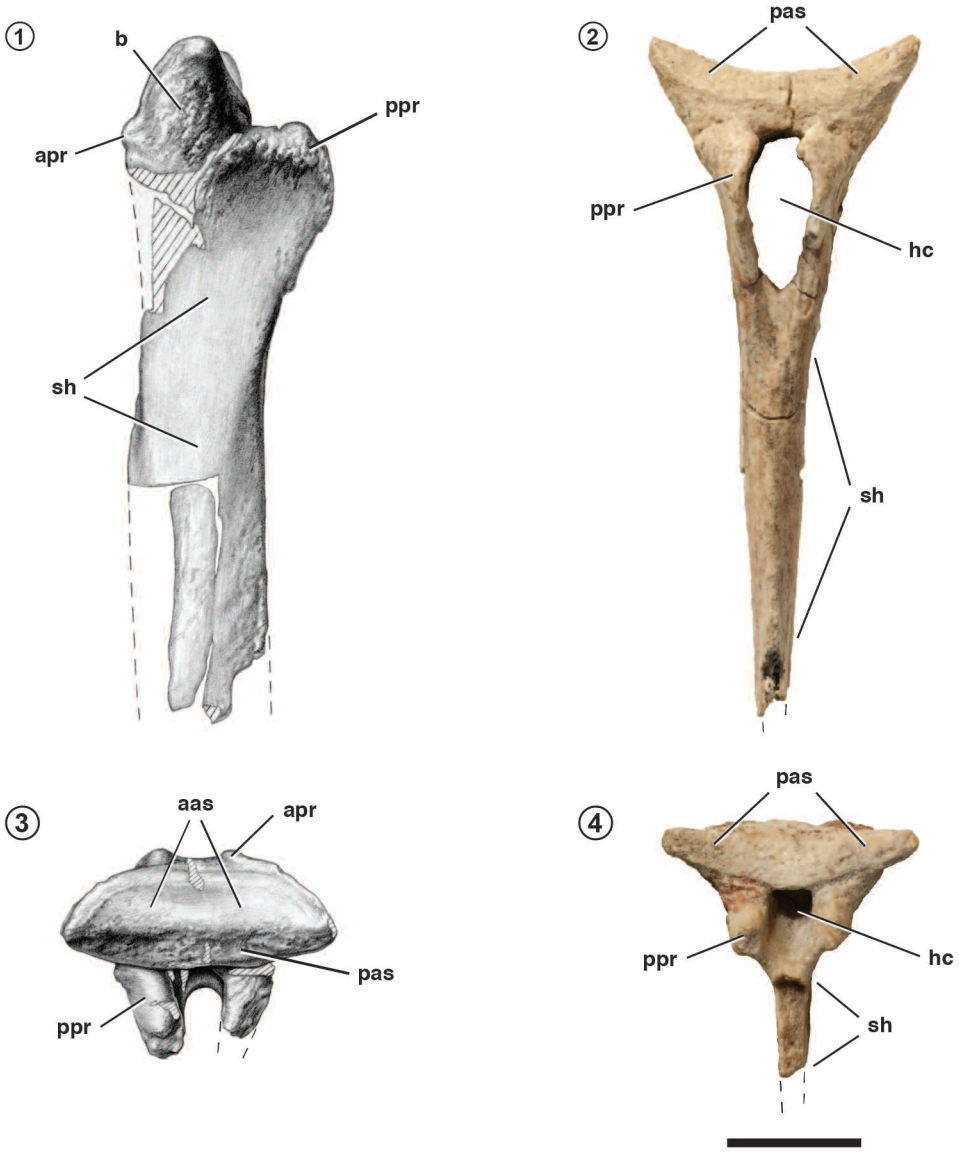

Figure 3. 1–2, ***Afromimus tenerensis*** gen. et sp. nov., **MNBH GAD**112. Chevron ?5; **1,** drawing of left lateral view; **2,** posterior view. **3-4,** ***Afromimus tenerensis*****, MNBH GAD**112. Chevron ?12; **3,** drawing of proximal view; **4,** posterior view. Dashed line indicates a missing margin. Abbreviations: **aas,** anterior articular surface; **apr,** anterior process; **b,** base; **hc,** haemal canal; **pas,** posterior articular surface; **ppr,** posterior process; **sh,** shaft. Scale bar= 1 cm.

Table 1 – Measurements of the axial bones of **Afromimus tenerensis** *gen. et sp. nov., (MNBH GAD112). The position (number) of caudal vertebrae and chevrons is approximate. Abbreviations: CA, caudal vertebra; Ch, chevron. Measurements are in millimeters; parentheses indicate estimated measurement.*

Bone	Dimension	Measurement
CA15	*posterior centrum face, width*	*32.1*
	posterior centrum face, midline height	*15.3*
	posterior centrum face, maximum height	*16.9*
CA16	*centrum length*	*52.9*
	posterior centrum face, width	*31.4*
	posterior centrum face, midline height	*14.9*
	posterior centrum face, maximum height	*16.8*
CA18	*centrum length*	*(49.4)*
CA20	*centrum length*	*50.9*
	posterior centrum face, width	*28.9*
	posterior centrum face, midline height	*13.9*
	posterior centrum face, maximum height	*14.5*
CA22	*posterior centrum face, width*	*(26.4)*
	posterior centrum face, midline height	*11.8*
	posterior centrum face, maximum height	*11.9*
CA24	*centrum length*	*(40.0)*
	posterior centrum face, width	*20.9*
	posterior centrum face, midline height	*10.6*
	posterior centrum face, maximum height	*10.9*
CA27	*centrum length*	*39.6*
	posterior centrum face, width	*22.1*
	posterior centrum face, midline height	*(9.3)*
	posterior centrum face, maximum height	*10.7*
Ch5	*articular base, maximum width*	*20.5*
	articular base, midline length	*7.2*
	posterior process, length	*7.2*
	hemal canal, height	*11.2*
	hemal canal, width	*5.1*
Ch12	*articular base, maximum width*	*19.6*
	articular base, midline length	*7.0*
	posterior process, length	*3.6*
	hemal canal, height	*3.8*
	hemal canal, width	*3.4*

tibial shaft distal to the lateral condyle, a rugose attachment surface on the fibula posterior to the tibial crest, trough on the anteromedial aspect of the fibular shaft ventral to the anterior trochanter, rugose texture on non-articular surfaces of pre- and postzygapophyses of mid caudal vertebrae, elevated zygapophyseal facets on pre-and postzygapophyses of mid caudal vertebrae, and fused pedicels on anterior chevrons that are less than one half as long anteroposteriorly as broad transversely.

DESCRIPTION

The following description is based on the holotypic and only known specimen (MNBH GAD112).

Axial skeleton (Figs. 1–3; Tab. 1)

Caudal vertebrae **(Figs. 1, 2).** Seven partial caudal vertebrae and fragments of others are preserved from the distal one half of the tail. The anterior- and posteriormost vertebrae are tentatively identified as CA ?15 and CA ?27, based on other ornithomimosaurs (*e.g.*, *Harpymimus*; Kobayashi and Barsbold, 2005b).

CA ?16 is tentatively located just anterior to the transition point, given its reduced transverse process and relatively short prezygapophyses (Fig. 1). The amphicoelous centrum is twice as broad as tall (Fig. 1.4–5). In posterior view, the centrum face is peanut-shaped, the median embayments dorsally and ventrally marking the neural canal

Table 2 – Four stem-based phylogenetic definitions used in this paper.

Taxon	*Phylogenetic Definition*	*Definitional Author*
Ornithomimiformes	*The most inclusive clade containing* **Ornithomimus edmontonicus** *Sternberg, 1933 but not* **Passer domesticus** *(Linnaeus, 1758).*	*Sereno, 2005b*
Ornithomimosauria Barsbold, 1976	*The most inclusive clade containing* **Ornithomimus edmontonicus** *Sternberg, 1933 but not* **Tyrannosaurus rex** *Osborn, 1905,* **Shuvuuia deserti** *Chiappe* et al.*, 1998,* **Therizinosaurus cheloniformis** *Maleev, 1954,* **Oviraptor philoceratops** *Osborn, 1924,* **Troodon formosus** *Leidy, 1856,* **Passer domesticus** *(Linnaeus, 1758).*	*Sereno, 2005b*
Ornithomimoidea Marsh, 1890	*The most inclusive clade containing* **Ornithomimus edmontonicus** *Sternberg, 1933 but not* **Nqwebasaurus thwazi** *de Klerk* et al.*, 2000,* **Tyrannosaurus rex** *Osborn, 1905,* **Shuvuuia deserti** *Chiappe* et al.*, 1998,* **Therizinosaurus cheloniformis** *Maleev, 1954,* **Oviraptor philoceratops** *Osborn, 1924,* **Troodon formosus** *Leidy, 1856,* **Passer domesticus** *(Linnaeus, 1758).*	*this paper, modified from Sereno, 1999a, 1999b)*
Ornithomimidae Marsh, 1890	*The most inclusive clade containing* **Ornithomimus edmontonicus** *Sternberg, 1933 but not* **Garudimimus brevipes** *Osmólska* et al.*, 1972,* **Harpymimus okladnikovi** *Barsbold and Perle, 1984,* **Shenzhousaurus orientalis** *Ji* et al.*, 2003,* **Pelecanimimus polyodon** *Perez-Moreno* et al.*, 1994.*	*Sereno 2005b*

and principal articular contacts of the chevron, respectively. The ventral embayment, which is shallower than the dorsal embayment, is absent in more posterior caudal vertebrae (Fig. 2.4), although the centrum face retains very broad proportions. The peanut-shaped centrum faces of mid caudal vertebrae in *Afromimus* and other ornithomimosaurs (Osmólska *et al.*, 1972: pl. 53, fig. 1d; Longrich, 2008: fig. 7) are distinctive but not yet recognised as an ornithomimosaur synapomorphy. The centrum faces of mid caudal vertebrae are subcircular in ceratosaurs or basal tetanurans, such as *Masiakasaurus* (Carrano *et al.*, 2002), *Elaphrosaurus* (Rauhut and Carrano, 2016), *Deltadromeus* (Sereno *et al.*, 1996), alvarezsauroids (Novas, 1997), and therizinosaurids (Zanno, 2010). The centra show no evidence of pleurocels or other invaginations and are composed of fairly dense cancellous bone. Several of the vertebrae (CA ?18, ?22, ?24), however, show a blind, cylindrical cavity in the center of the centrum that narrows in diameter in the more distal caudal vertebrae. In CA ?24 the cavity is slightly greater in diamter than the neural canal (Fig. 2.3).

The transverse process of CA ?16 is a low, rugose, horizontal ridge shifted slightly posterior to the mid point of the centrum (Fig. 1.1). The ridge is lower, although still rugose, in CA ?20, and becomes smooth in CA ?27. In ventral view, two prominent, parasagittal, rugose crests course between the attachment surfaces for the chevrons (Fig. 1.3). They are prominent in CA ?16, very low in CA ?20 and absent by CA ?24 (Fig. 2.3). In CA ?16, these ridges are joined posteriorly by a median, subtriangular, rugose attachment surface (Fig. 1.3) located adjacent to the smooth centrum rim for articulation with the chevron (Fig. 1.5). An accessory rugose ridge is present below the transverse process in CA ?16 as seen in lateral view, running along the posterior one half of the centrum, terminating in a low process (Fig. 1.1). A concave rugose depression is present ventral to this process (Fig. 1.1, 1.3). This depression is present as far distally as CA ?27, where it is smooth.

The neurocentral suture is completely coossified in all preserved caudal vertebrae. The neural spine is developed as a low crest that dissipates distally in CA ?16 (Fig. 1.2). The spine is abraded in CA ?24 (Fig. 2.2) but remains as a low crest in CA ?27. The diameter of the neural canal is small relative to the centrum and neural arch (Figs. 1.5, 2.4) as in other ornithomimids (Longrich, 2008).

The form and articulation of pre-and postzygapophyses are distinctive. In CA ?16 the prezygapophyses are only

modestly lengthened, arching anterodorsally beyond the anterior centrum face in lateral view (Fig. 1.1). The lateral surface is rugose, an autapomorphy for the species (Fig. 1.1). The ventromedially inclined medial surface has a distinct, raised articular facet for an opposing smooth surface on the postzygapophysis (Fig. 1.2). The smooth oval facet has its major axis inclined posteroventrally and is about twice as long (10 mm) as wide (5 mm). The portion of the process distal to the articular facet is very gently cupped and clearly was separated slightly from the opposing surface of the opposing postzygapophysis (Fig. 1.2). The portion of the process proximal to the facet is developed into a rimmed depression to receive the distal end of the opposing postzygapophysis (Fig. 1.2). The same paired, rimmed depressions are present in CA ?24, although shallower in depth (Fig. 2.2). The postzygapophyses of mid caudal vertebrae, thus, are lodged within a rimmed fossa that interlocks adjacent vertebrae, a condition present in *Sinornithomimus* and more advanced ornithomimids (Longrich, 2008).

The postzygapophyses are relatively short, extending only a short distance beyond the posterior centrum face in CA ?16 (Fig. 1.1). In CA ?26 and CA ?27, the postzygapophyses probably do not extend beyond the posterior centrum face (Fig. 2.1). Like the prezygapophyses, the lateral surface of the postzygapophyses is rugose and each has a well delineated, smooth articular facet near the end of the process (Fig. 1.1, 1.3, 1.5). In CA ?16 the articular facet is subtriangular and nearly flat, its medial corner rounded to fit against the cupped medial edge of the opposing prezygapophysis. The tip of the postzygapophysis tapers to a blunt point along its medial edge, which would have lodged within a an accommodating fossa on the neural arch of the succeeding caudal (Fig. 1.2).

Chevrons (Fig. 3). The proximal part of two chevrons, tentatively identified as Ch ?5 and Ch ?12, are preserved from the anterior one half of the tail. The pedicels of both chevrons are fused over the haemal canal to form an anteroposteriorly narrow, crescent-shaped base (Fig. 3.3–4).

Ch ?5 has a long, parallel-sided shaft (Fig. 3.1) typical of chevrons associated with the proximal fifteen caudal vertebrae (Kobayashi and Barsbold, 2005b). Very little curvature is apparent in the preserved proximal portion of the shaft in lateral view, which is marked by a rugosity below the haemal canal (Fig. 3.1). The posterior processes are much larger than the anterior processes and are better developed than in *Harpymimus* (Kobayashi and Barsbold, 2005b). A capacious, oval haemal canal is enclosed (Fig. 3.2). The second chevron, estimated to be the 12th, preserves the base and a portion of the shaft. The fused base and much larger anterior processes are similar to the pattern present in Ch ?5 (Fig. 3.3). The shaft is not well enough preserved to know its shape or length. The haemal canal is relatively much smaller than on Ch ?5 and passes through the base at an acute angle to the axis of the shaft (Fig. 3.4).

Hind limb (Figs. 4–10; Tab. 3)

Tibia (Figs. 4-6). The right tibia lacks most of the condyles proximally and the medial corner distally. In lateral view of the proximal end, the cnemial crest arches from its broken end proximally to the shaft (Fig. 5.3). Although the complete profile and proximal projection of the cnemial crest is unknown, the trough between the crest and lateral condyle (or tibial incisure) is very broad in anterior or lateral views (Figs. 4.1, 5.4). The posterior portion of the lateral condyle is preserved, its ventral edge delineated from the shaft as in *Sinornithomimus* (LH PV7) and *Gallimimus* (Osmólska *et al.*, 1972: pl. 47, fig. 3).

The fibular crest is relatively shorter and narrower than in *Sinornithomimus* (LH PV7) and *Gallimimus* (Osmólska *et al.*, 1972: pl. 51, fig. 2). Unlike these two genera, the fibular crest in *Afromimus* dissipates ventrally before the cnemial crest and is too short transversely to contact and overlap the opposing tibial crest of the fibula in natural artifulation (Fig. 4.1–2). The fibular crest in *Afromimus*, in addition, increases in depth toward its ventral, rather than dorsal, end (Figs. 4.1). Another unusual feature is the presence of a large elliptical attachment scar, crossed by spaced linear rugosities, located on the posterolateral aspect of the proximal tibial shaft just posterior to the fibular crest (Fig. 4.2). The fibula also has a large rugose attachment surface proximally (Fig. 7.4), but this surface is positioned at a distance from the attachment scar on the tibia, when these bones are brought into articulation (Fig. 4.2). The tibial attachment scar, therefore, is probably the origin of the tibialis anterior muscle for flexion of the pes (Carrano and Hutchinson, 2002). The presence or absence of these features in *Nqwebasaurus* is not known.

The tibial shaft is anteroposteriorly compressed, flatter

anteriorly than posteriorly, and gently laterally bowed (Fig. 5.1–2; Tab. 3). The lateral curvature of the shaft is more marked than in *Sinornithomimus* (LH PV7), *Beishanlong* (Makovicky *et al.*, 2009: fig. 3d) or *Gallimimus* (Osmólska *et al.*, 1972: pl. 47, fig. 3). A groove near the ventral end of the fibular crest courses ventrally to an inset nutrient foramen in the upper one third of the shaft (Fig. 5.4). From the lip of the foramen to the lateral malleolus, the lateral shaft edge is flattened and subtely textured for contact with the fibular shaft. Along the anterior side of the articular surface is smooth shallow tough, which extends ventrally to the articular surface for the astragalus (Fig. 4.3).

The distal end of the tibia expands transversely to form the flat lateral malleolus, which is partially coossified with

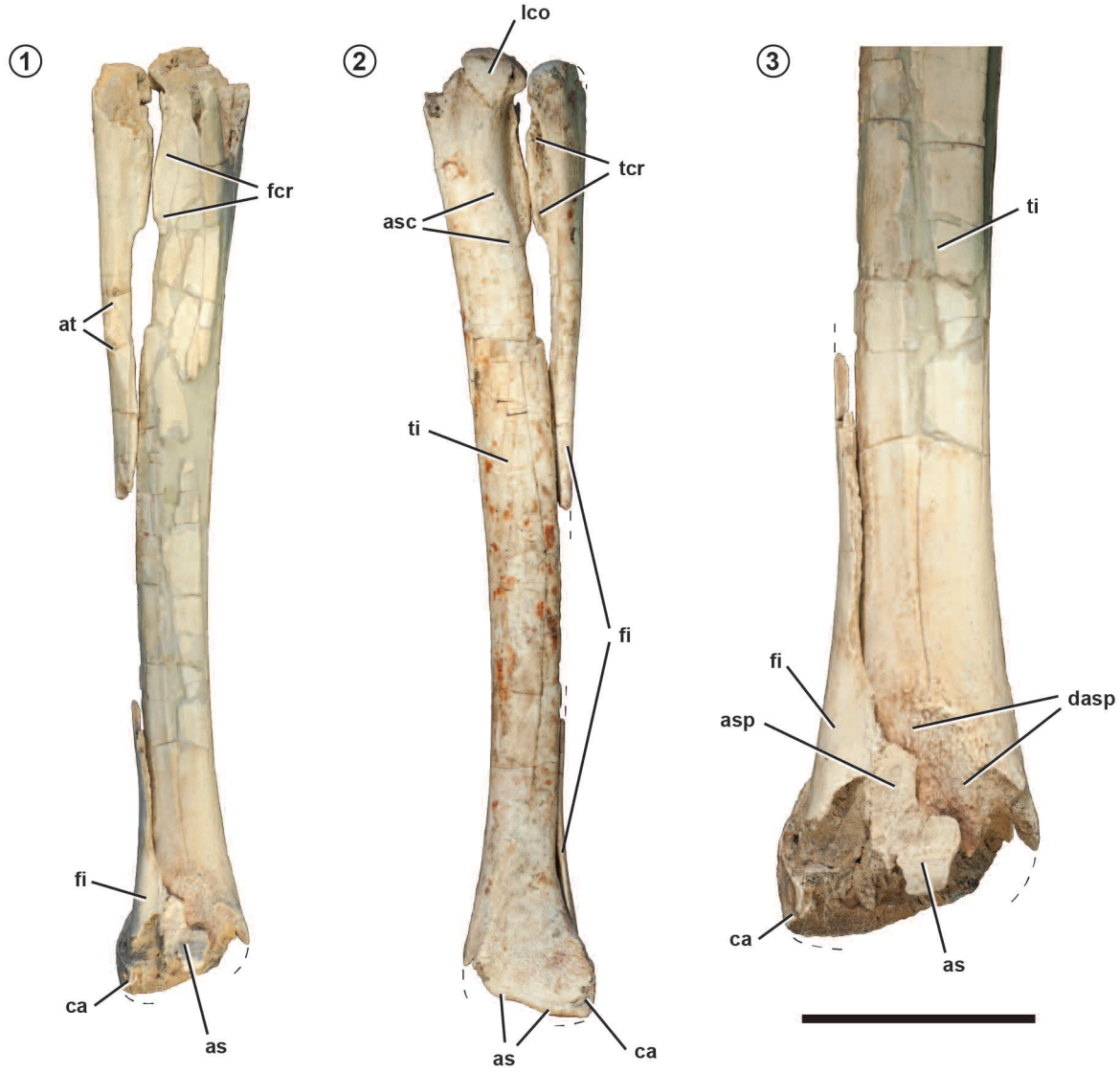

Figure 4. 1–3, ***Afromimus tenerensis*** gen. et sp. nov., **MNBH GAD**112. Right tibia and partial fibula, astragalus and calcaneum; **1,** anterior view; **2,** posterior view; **3,** anterior view of distal end. Dashed line indicates a missing margin. Abbreviations: **as,** astragalus; **asc,** attachment scar; **asp,** ascending process; **at,** anterior trochanter; **ca,** calcaneum; **dasp,** depression for the ascending process; **fcr,** fibular crest; **fi,** fibula; **lco,** lateral condyle; **tcr,** tibial crest; **ti,** tibia. Scale bar= 10 cm in 1–2 and 5 cm in 3.

Table 3 – Measurements of the appendicular bones of **Afromimus tenerensis** *gen. et sp. nov. (MNBH GAD112). Limb bones are from the right side. Abbreviations: II, III, pedal digits II, III. Measurements are in millimeters; parentheses indicate estimated measurement.*

Bone	Dimension	Measurement
Tibia	*length*	*404.5*
	mid shaft, transverse width	*30.9*
	mid shaft, anteroposterior depth	*23.6*
	distal end, width	*(58.7)*
Fibula	*length*	*(389.8)*
	proximal end to apex of anterior trochanter, length	*120.7*
	distal shaft, transverse width	*5.0*
	distal shaft, anteroposterior depth	*10.0*
	distal end, transverse width	*17.5*
Astragalus	*ascending process, height*	*33.1*
	ascending process base, width	*35.4*
Calcaneum	*lateral face, dorsoventral length*	*18.8*
	lateral face, anteroposterior depth	*(19.2)*
Phalanx II-2	*distal condyles, width*	*(21.4)*
Phalanx III-1	*proximal articular surface, height*	*19.5*
	proximal articular surface, maximum width	*21.6*
Ungual II-3	*length*	*32.2*
	proximal articular surface, height	*(19.0)*
	proximal articular surface, maximum width	*13.9*

the astragalus and calcaneum (Fig. 4.3), a condition unknown in ornithomimosaurs but variably present in noasaurids and alvarezsauroids (Carrano *et al.*, 2002; Novas, 1997). The lateral malleolus in *Afromimus* (Fig. 6) extends ventrally and laterally to a greater extent than in *Sinornithomimus* (LH PV7) and *Gallimimus* (Osmólska *et al.*, 1972: pl. 51, fig. 2). In anterior view, it extends laterally approximately one third of the width of the distal end (Fig. 6.1–2). In posterior view, the suture with the astragalus is angled more strongly ventrolaterally than in other onithomimosaurs (Fig. 6.3–4). A rugose texture covers the posterior aspect of the distal end of the tibia (Fig. 6.3–4).

The articular surface for the astragalus is rugose and inset along its medial edge (Fig. 6). A raised rugose lip, termed the "medial buttress" (Galton and Molnar, 2005), clearly demarcates the medial margin of the ascending process as it crosses the tibial shaft from the medial side at the ankle joint. The medial buttress is low in *Harpymimus* (Kobayashi and Barsbold, 2005b) and poorly developed or absent in most other ornithomimosaurs (Allain *et al.*, 2014). The ascending process is neither as broad nor as tall as in *Sinornithomimus* (LH PV7) or *Gallimimus* (Osmólska *et al.*, 1972: pl. 47, fig. 3), where it extends to the medial margin of the tibia. The medial malleolus in *Afromimus* is prominent anteriorly, its distal margin eroded away (Fig. 6). The preserved portion of the medial malleolous shows that the medial edge of the ascending process of the astragalus is offset from the medial margin of the tibia. This condition is similar to that described in *Nqwebasaurus* below and distinctly more primitive than that in all other ornithomimosaurs, including the oldest European ornithomimosaurs from England and France (Galton and Molnar, 2005; Allain *et al.*, 2014) and the oldest Asian ornithomimosaurs preserving the distal tibia (*Harpymimus*, Kobayashi and Barsbold, 2005b; *Beishanlong*, Makovicky *et al.*, 2009). In these ornithomimosaurs, the flattened articular surface for the astragalar ascending process covers all but the most slender edge along the medial margin of the distal tibia.

Fibula (Figs. 4, 7, 8). The right fibula is missing the anterior portion of the proximal condyle and the central one third of its shaft. In anterior view, the tibial crest and anterior trochanter are separated by approximately 2 cm of shaft (Fig. 7.1), whereas the two are joined in more derived ornithomimosaurs such as *Sinornithomimus* (LH PV7) or *Galli-*

mimus (Osmólska *et al.*, 1972: pl. 47, fig. 3). The more distal position of the anterior trochanter in *Afromimus* appears to be the reason for separation of the two crests. In posterior view, the prominence and subrectangular profile of the tibial crest is visible (Fig. 7.2). In lateral view, striations mark two areas of muscle attachment, the first a larger triangular area in the center of the shaft near the proximal end and the second a smaller triangular surface ventral to the posterior extemity of the proximal end (Fig. 7.3).

The anterior trochanter, the insertion for the iliofibularis muscle (Carrano and Hutchinson, 2002), is prominently developed as a rugose process (Fig. 7.3, 7.4). In other ornithomimosaurs, the anterior trochanter is poorly developed as a prominence or gentle bend in the anterior margin of the fibular shaft. There is no noticeable trochanter, for example, in *Nqwebasaurus*, although it is only one third the body

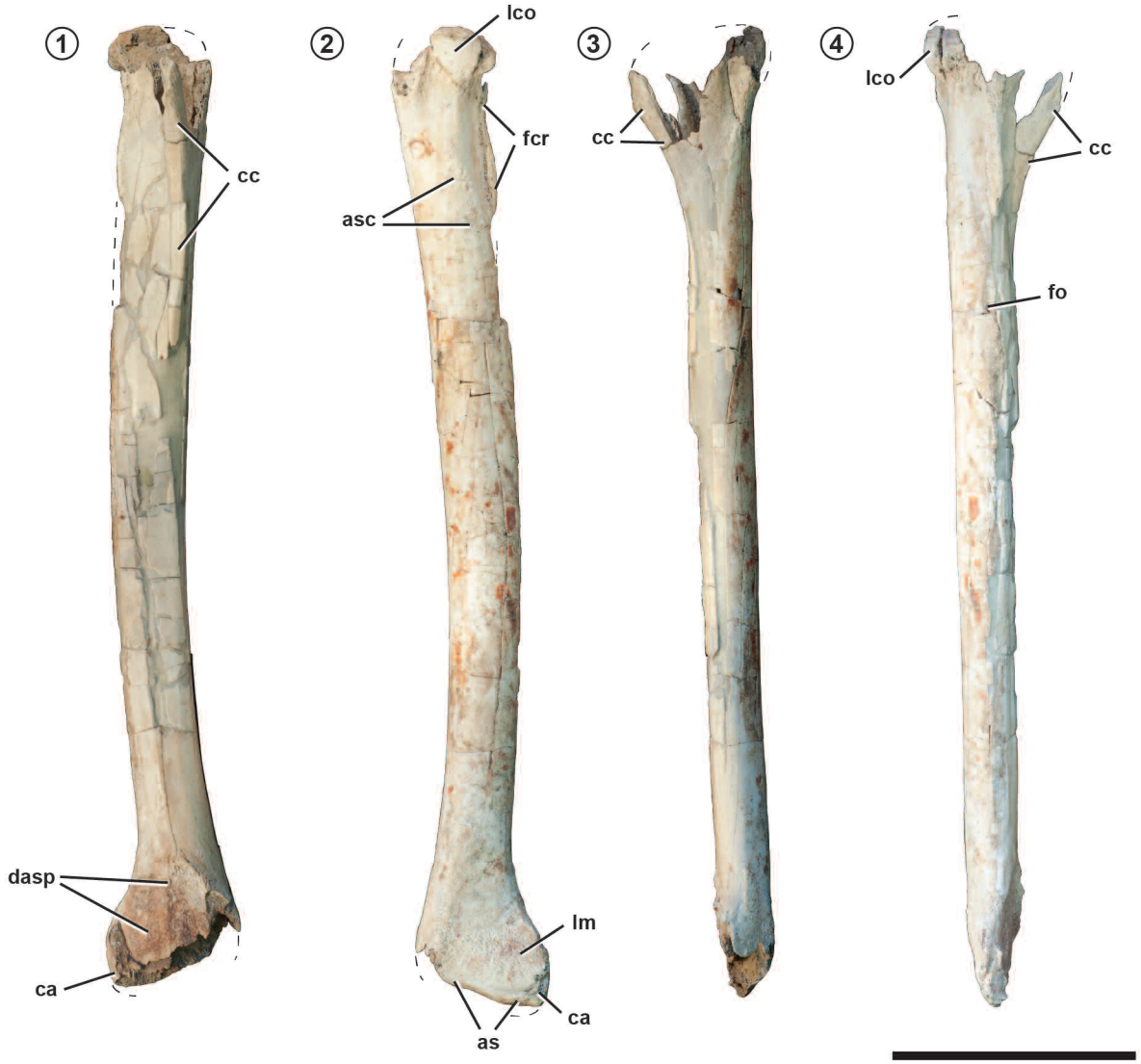

Figure 5. 1–3, ***Afromimus tenerensis*** gen. et sp. nov., **MNBH GAD**112. Partial right tibia with small fragments of adjacent bones; **1,** anterior view; **2,** posterior view; **3,** medial view; **4,** lateral view. Dashed line indicates a missing margin. Abbreviations: **as,** astragalus; **asc**, attachment scar; **asp,** ascending process; **at,** anterior trochanter; **ca,** calcaneum; **cc,** cnemial crest; **dasp,** depression for the ascending process; **fi,** fibula; **fcr,** fibular crest; **fo,** foramen; **lco,** lateral condyle; **lm,** lateral malleolus. Scale bar= 5 cm in 1–2 and 2.5 cm in 3.

size of *Afromimus*. The same holds, nevertheless, for the large-bodied, stocky-limbed ornithomimosaur *Beishanlong* (Makovicky *et al.*, 2009). A large fibular fossa is present on the medial aspect of the proximal fibula in *Afromimus* (Fig. 7.2, 7.4). Its dorsal margin formed by a posterodorsally inclined strut of bone, and the fossa opens medially and posteriorly. The dorsal portion of the fossa is deeply invaginated. Ventrally the fibular fossa extends smoothly onto the shaft and is continuous with an unusual trough running anteromedial to the anterior trochanter (Fig. 7.4). The fibular shaft distal to the anterior trochanter is slightly transversely compressed. A rugose attachment surface is present along the anterior margin of the tibial crest and again on the shaft more distally, suggesting that the fibular shaft was appressed against the tibial shaft along its length. The form of both the anterior trochanter and fibular fossa closely resemble the condition in the noasaurid *Masiakasaurus* and in the basal coelurosaur *Deltadromeus* (Carrano *et al.*, 2011: fig. 23; Sereno *et al.*, 1996: fig. 3G). A deep, posteriorly open fibular fossa also characterizes some basal tetanurans such

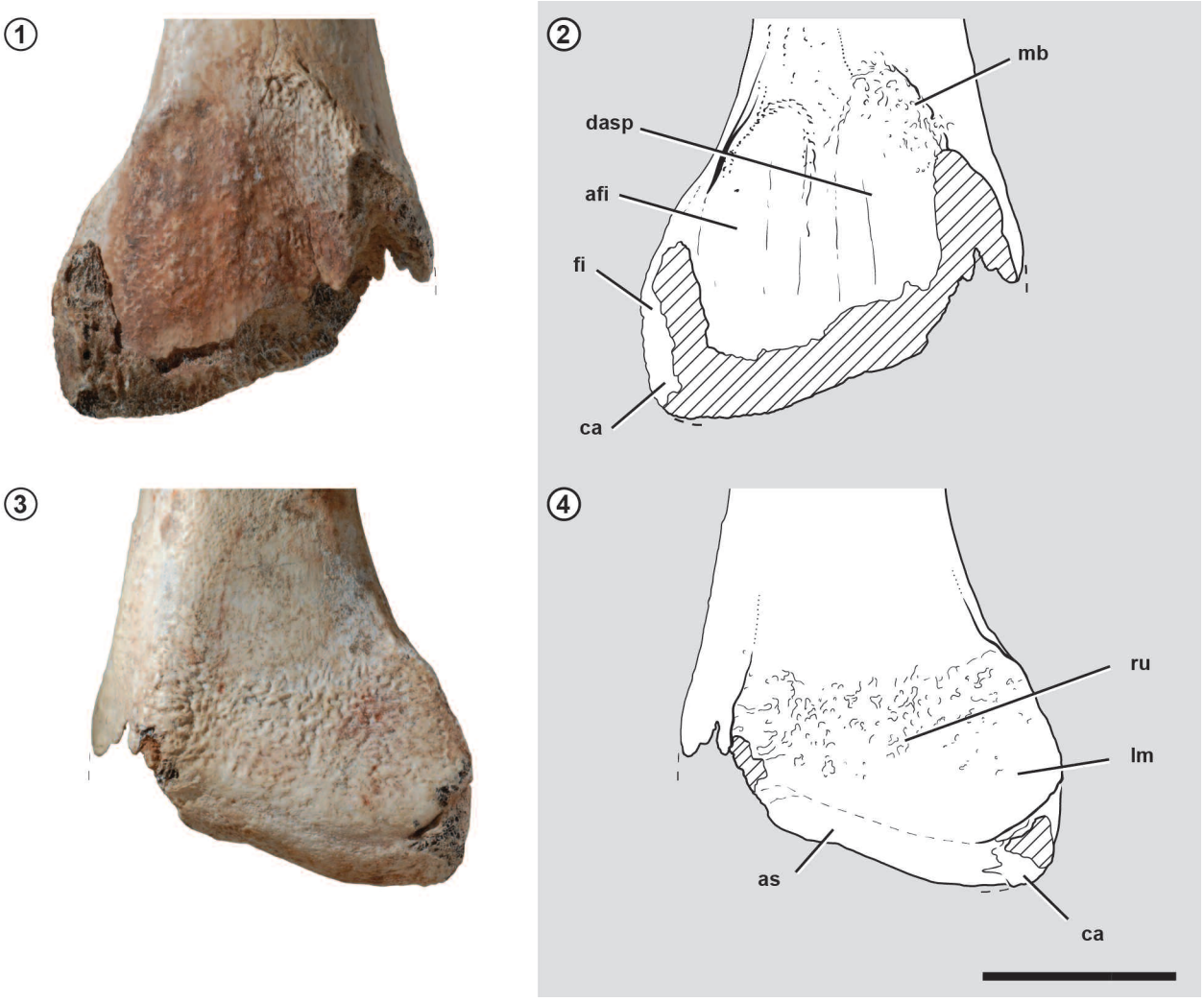

Figure 6. 1–4, ***Afromimus tenerensis*** gen. et sp. nov., **MNBH GAD**112. Distal right tibia and partially coossified fragments of the distal fibula, astragalus and calcaneum; **1–2,** anterior view; **3–4,** posterior view. Hatching indicates a broken surface; dashed line indictaes a missing margin (or fused suture over bone). Abbreviations: **afi,** articular surface for the fibula; **as,** astragalus; **ca,** calcaneum; **dasp,** depression for the ascending process; **fi,** fibula; **lm,** lateral malleolus; **mb,** medial buttress; **ru,** rugosity. Scale bar= 3 cm

as *Neoventor* (Brusatte *et al.*, 2008) and other basal coleurosaurs such as *Tyrannosaurus* (Brochu, 2003). The condition of the fibular fossa in basal ornithomimosaurs is best known in *Beishanlong*, which has a similarly deep fossa (Makovicky *et al.*, 2009).

The distal fibular shaft is transversely expanded, measuring approximately 10 mm in width and 5 mm in depth (Fig. 8). The distal end of the fibula is transversely broad for a coelurosaur (Fig. 8.1), proportionately broader than in *Sinornithomimus* (LH PV7), *Beishanlong* (Makovicky *et al.*, 2009) or *Gallimimus* (Osmólska *et al.*, 1972: pl. 47, fig. 3). Marked transverse expansion of the distal end of the fibula also may occur in *Nqwebasaurus* (see below) but is absent in other ornithomimosaurs. The distal fibular shaft articulates against the tibial shaft, a medial rugosity opposing one on the tibial shaft (Fig. 8.2, 8.5). Although much of the distal condyle is abraded away in anterior view (Fig. 8.1, 8.4), a fused suture is preserved with the astragalar ascending process medially and the calcaneum distally (Fig. 8.1, 8.3, 8.4, 8.6).

Astragalus (Figs. 4, 6, 8). Only the coossfied posterior edge and the medial portion of the ascending process of the right astragalus are preserved. The contact between the ascending process and tibia is not fused, which has allowed their disarticulation (Fig. 8). The edge of the condylar surface sug-

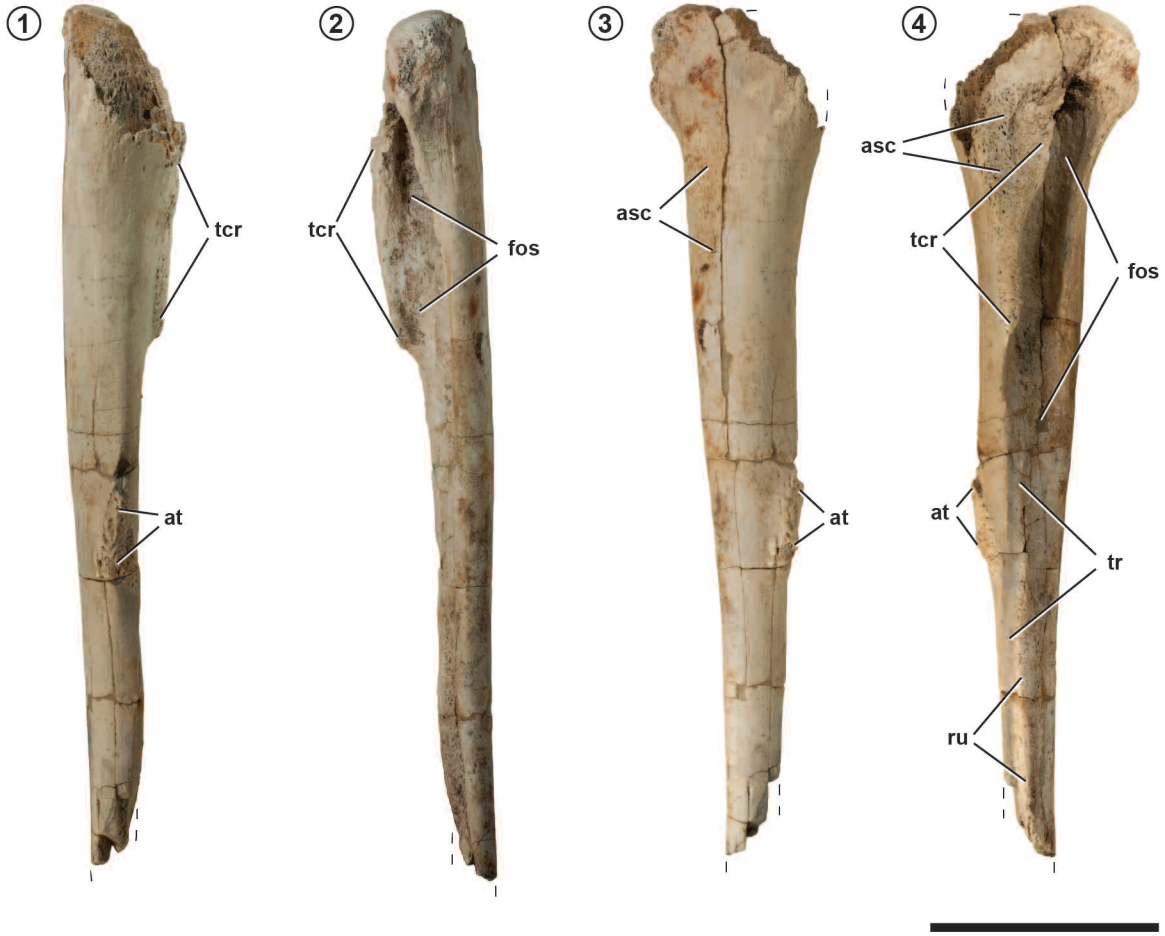

Figure 7. 1–4, ***Afromimus tenerensis*** gen. et sp. nov., **MNBH GAD**112. Proximal end of the right fibula; **1,** anterior view; **2,** posterior view; **3,** lateral view; **4,** medial view. Dashed line indicates a missing margin. Abbreviations: **at,** anterior trochanter; **asc,** attachment scar; **fos,** fossa; **ru,** rugosity; **tcr,** tibial crest; **tr,** trough Scale bar= 5 cm.

gests that it had the usual saddle shape (Fig. 6.3–4). A medial buttress marks the edge of the ascending process on the medial malleolus of the tibia (Fig. 6.1–2). The ascending process in *Afromimus* (Fig. 4.3) is not as broad relative to the distal end of the tibia as in *Harpymimus* (Kobayashi and Barsbold, 2005b), *Sinornithomimus* (LH PV7) or *Gallimimus* (Osmólska *et al.*, 1972: pl. 47, fig. 3). Nonarticular surfaces of the distal end of the tibia are visible to each side of the contact for the stragalus (Fig. 6.1–2) as in *Nqwebasaurus* (Choiniere *et al.*, 2012: fig. 13). The ascending process tapers to a narrow tip alongside the fibula, as suggested by a sutural edge on the fibula (Fig. 8.1, 8.4) and a faint articular impression on the distal end of the tibia (Figs. 4.3, 6.1–2).

Calcaneum (Figs. 4, 6, 8). The right calcaneum is preserved in two pieces, a fragment coossified with the distal end of the tibia and astragalus that preserves some of its ventral and lateral surface (Fig. 6) and a second fragment coossified with the distal end of the fibula that preserves some of its lateral surface (Fig. 8). The coossified junction between the calcaneum and astragalus is exposed in posterior view with a prong-shaped medial process on the calcaneum still discernable (Fig. 6.3–4). More of the calcaneum is exposed in anterior and posterior views of the distal end of the ankle joint in *Afromimus* than in *Beishanlong* (Shapiro *et al.*, 2003), *Sinornithomimus* (LH PV7) or *Gallimimus* (Osmólska *et al.*, 1972, pl. 47, fig. 3). In these ornithomimosaurs, the calcaneum is visible in anterior and posterior views only as a narrow, vertical rounded edge.

Pedal phalanges (Figs. 9, 10). The proximal end of a hollow pedal phalanx is preserved (Fig. 9.1–2). The heel of its base projects proximally beyond the apex where flexors attached (Fig. 8.1). The dorsoventrally concave proximal articular surface is undivided, suggesting it is a proximal phalanx that articulated with the undivided distal condyle of a metatarsal. Its symmetry in proximal view (Fig. 9.2) suggests it pertains to pedal digit III, rather than pedal digits II or IV, as pedal phalanx III-1.

The distal end of another pedal phalanx is preserved (Fig. 9.3, 9.5). Its shaft is hollow, its distal condyles divided, and the dorsal aspect of its distal end is marked by a well developed dorsal extensor depression (Fig. 9.3). Although slightly enlarged from weathering, one of its collateral ligament pits is larger than the other (Fig. 9.4). In many theropods, the collateral ligament pits of pedal digit III are symmetrical, whereas those on digits II and IV are asymmetrical. For digits II and IV, the ligament pit on the internal side (*i.e.*, the side facing digit III) has a greater diameter than its opposite. If this phalanx, like the crus, pertains to the right hind limb, it pertains to pedal phalanx II-2.

One ungual is preserved with an asymmetric proximal articular surface (Fig. 10.3). Its asymmetry suggests it pertains to pedal digit II or IV, rather than digit III. One side of the ungual is deeper than the other, its ventral attachment groove closer to the ventral margin of the ungual (Fig. 10.1). The asymmetry is related to the tilt of the sagittal plane of the ungual, the deeper side more fully exposed in dorsal view. A completely preserved and articulated pes of *Sinornithomimus* (LH PV7) shows that the deepr sides of the unguals of pedal digits II and IV face away from the central axis of the pes; the sagittal plane of each ungual tilts toward that of pedal digit III. If the preserved ungual, like the crus, pertains to the right hind limb, its asymmetry identifies it as the ungual of pedal digit II.

In presumed medial view (Fig. 10.1), the ventral margin of the ungual is straight as in all ornithomimosaurs except the stocky-limbed *Beishanlong* (Shapiro *et al.*, 2003; Makovicky *et al.*, 2009). Breakage on the presumed medial side of the phalanx shows cancelous bone at the base and a smooth-walled, space that hollowed the distal two-thirds of the ungual. There are distinctive dorsal and ventral attachment grooves for the ungual sheath on both sides. On the presumed medial side, three foramina open in both grooves, the largest of which in each case is centrally located (Fig. 10.1). The dorsal attachment groove fades anteriorly toward the tip of the ungual. The ventral attachment groove extends from the ungual tip toward the proximal end, turning onto the ventral aspect of the ungual (Fig. 10.2). A very faint vertical groove is present, centered on a small foramen dorsal to the recessed flexor attachment surface (Fig. 10.1). Closer to the proximal articular surface, rugosities mark the lateral margin near the base of the ungual. On the shorter, presumed lateral (interdigital) side of the ungual, both dorsal and ventral attachment grooves are present although not as deeply incised as on the opposite side. The proximal articular surface is very weakly divided into two concavities for the distal condyles of the penultimate phalanx (Fig. 10.3).

The subquadrate attachment area for the flexor tendon

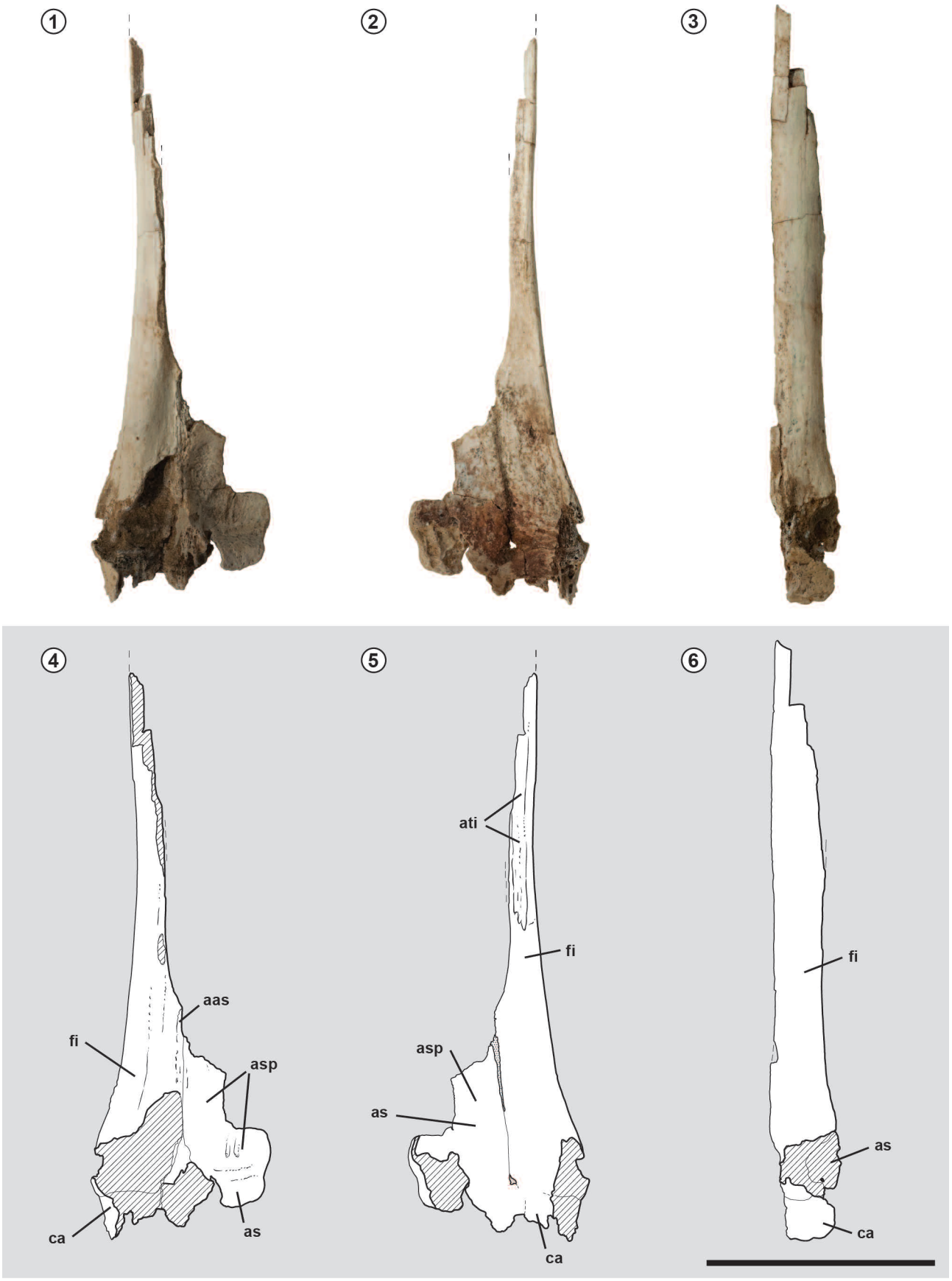
1
2
3
4
5
6
aas
fi
asp
ca
as
ati
fi
asp
as
ca
fi
as
ca

is recessed, as seen in lateral and ventral views (Fig. 10.1–2). The attachment surface is rugose with several deep pits, the central pit the deepest. Another pit is located between the limbs of a raised, V-shaped platform for the ungual sheath. The platform appears to support a subtriangular keratinized "hoof" that is limited to the distal two-thirds of the ungual. Because the sagittal plane of the ungual is canted away from the medial side of the ungual (Fig. 10.3), the medial edge of the ventral platform forms a sharp ridge, whereas the lateral (interdigital) edge is rounded (Fig. 10.3).

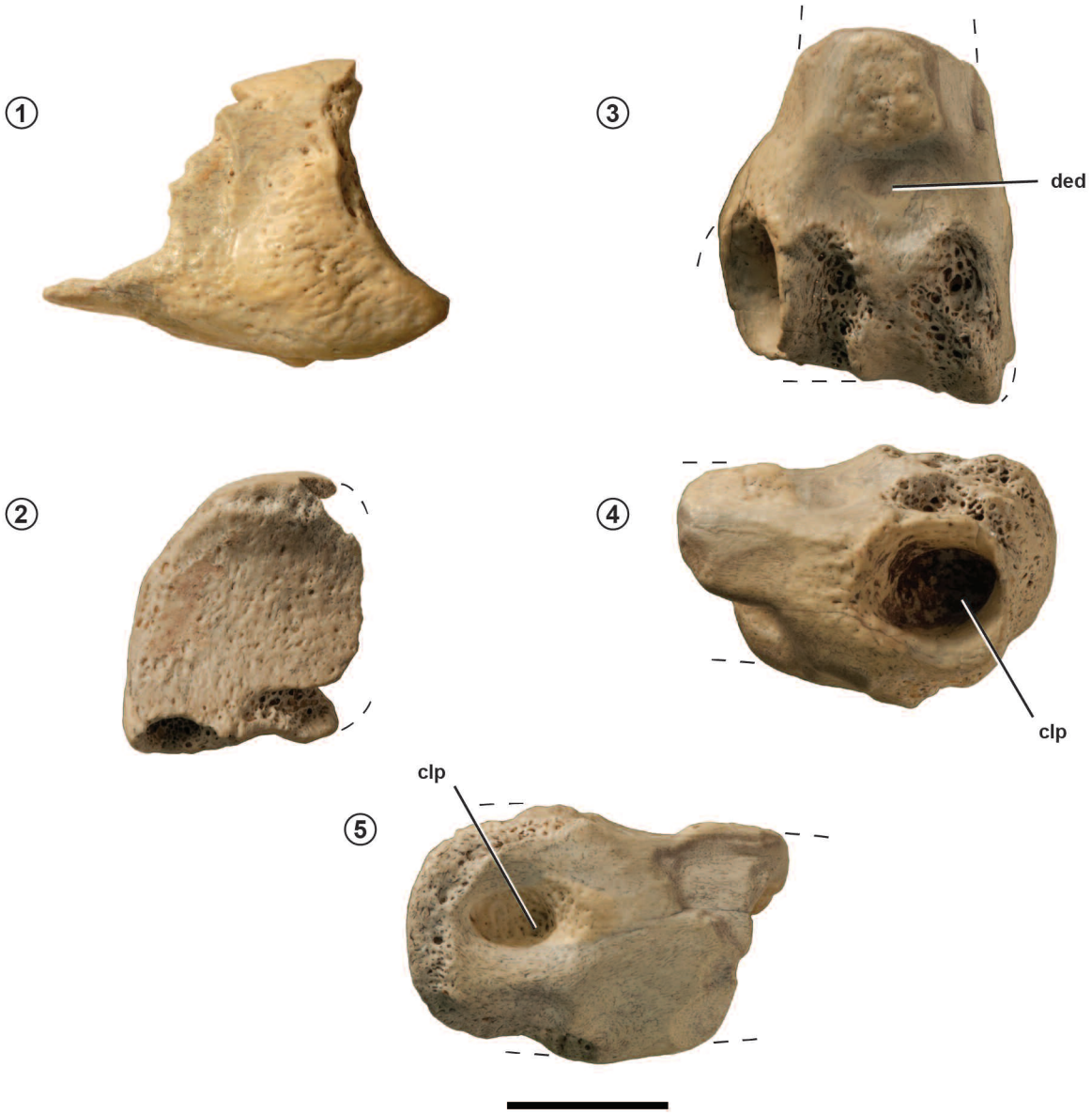

Figure 9. 1–5, ***Afromimus tenerensis*** gen. et sp. nov., **MNBH GAD**112. Proximal end of right pedal phalanx III-1; **1,** left lateral view; **2,** proximal view. **MNBH GAD**112. Distal end of pedal phalanx II-2; **3,** dorsal view; **4,** right lateral view; **5,** left lateral view. Dashed line indictaes a missing margin. Abbreviations: **clp,** collateral ligament pit; **ded,** dorsal extensor depression. Scale bar= 1 cm.

Figure 8. 1–6, ***Afromimus tenerensis*** gen. et sp. nov., **MNBH GAD**112. Distal right fibula and portions of the right astragalus and calcaneum; **1, 4,** anterior view; **2, 5,** posterior view; **3, 6,** lateral view. Hatching indicates a broken surface; dashed line indictaes a missing margin. Abbreviations: **aas,** attachment surface for the astragalus; **as,** astragalus; **asp,** ascending process of the astragalus; **ati,** attachment surface for the tibia; **ca,** calcaneum; **fi,** fubula. Scale bar= 5 cm.

Ornithomimosaurs including *Nqwebasaurus* have unrecurved unguals with a hoof-like ventral platform and recessed flexor attachment area. Only the the larger-bodied, stocky-limbed genera *Beishanlong* (Makovicky *et al.*, 2009) and *Deinocheirus* (Lee *et al.*, 2014) depart from this pattern, both showing some recurvature in lateral view. In *Beishanlong* a ventral platform is present, whereas in *Deinocheirus* the blunt-ended pedal unguals are modified for slower movement. A ventral platform, recessed flexor attachment area and reduced recurvature characterize the pedal unguals in noasaurids, although some recurvature is often retained (Novas and Bandyopadhyay, 2001; Carrano *et al.*, 2002). Fleet-footed alvarezsaurids, such as *Shuvuuia* (Suzuki *et al.*, 2002), lack the ventral platform but have pedal unguals with reduced recurvature. Some noasaurids (Novas and Bandyopadhyay, 2001; Carrano *et al.*, 2002) and alvsarezsaurids (Novas, 1997) exhibit two attachment grooves in pedal unguals as in *Afromimus*, although this condition appreas to be variable (Suzuki *et al.*, 2002).

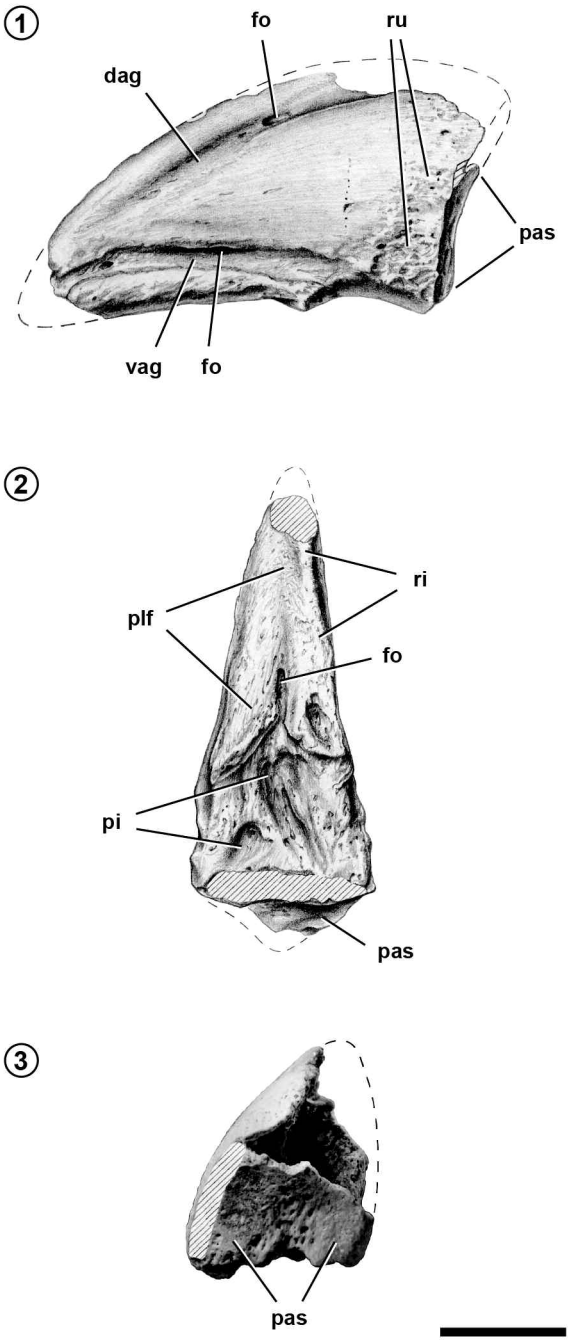

Figure 10. 1–3, ***Afromimus tenerensis*** gen. et sp. nov., **MNBH GAD**112. Drawings and photograph of right pedal ungual of digit II; **1,** medial view. **2,** ventral view; **3,** proximal view. Hatching indicates a broken surface; dashed line indictaes a missing margin. Abbreviations: **dag,** dorsal attachment groove; **fo,** foramen; **pas,** proximal articular surface; **pi,** pit; **plf,** platform; **ri,** ridge; **ru,** rugosity; **vag,** ventral attachment groove. Scale bar= 1 cm.

Nqwebasaurus de Klerk *et al.*, 2000
(Figures 11–24)

Type species. *Nqwebasaurus thwazi.*

Nqwebasaurus thwazi de Klerk *et al.*, 2000

Holotype. AM 6040, partial skull and postcranial skeleton preserving potions of the dorsal skull roof, braincase, sclerotic ring, mid to posterior cervical and isolated dorsal vertebrae, and portions of both girdles and fore and hind limbs (de Klerk *et al.*, 2000; Choiniere *et al.*, 2012).

Referred material. AM unnumbered, a femur, tibia and fibula of a second individual approximately one half the size of the holotype. The femur and tibia were found in the wall of the trench during collection of the holotypic skeleton, and the fibula was found under the skull bones of the holotype during preparation (W.J. de Klerk, pers. comm.). This material was not mentioned in previous studies.

Revised diagnosis. Basal ornithomimosaur with a well defined, elongate beveled edge on the orbital rim anterior to the postorbital, elongate dorsal centra (length approximately 3 times the centrum diameter), a crest on the distal shaft of metacarpal 1 (adjacent to metacarpal 2), metacarpal 1 with a lateral distal condyle twice as deep dorsoventrally as the medial condyle, unusually long unguals on manual digits II and III (the latter more than twice the length of the penultimate phalanx), and metatarsal 4 with a shaft ap-

proximately one half the transverse width of metatarsal 2.

Discussion. Of the features listed in the original diagnosis of *Nqwebasaurus thwazi* (de Klerk *et al.*, 2000: p. 325), two appear to stand as autapomorphies, namely an unusual ridge on the distal end of the shaft of metacarpal 1 and the large size of its lateral distal condyle. Although the lateral distal condyle of metacarpal 1 is larger than the medial condyle in *Herrerasaurus* (Sereno, 1994), *Eodromaeus* (Martinez *et al.*, 2011) and *Eoraptor* (Sereno *et al.*, 2012), in *Nqwebasaurus* the disparity between the condyles is pronounced. The lateral condyle is twice as deep dorsoventrally as the medial condyle (de Klerk *et al.*, 2000: fig. 4C). Metatarsal 4, likewise, has a considerably more slender shaft than metatarsal 2, whereas in other ornithomimosaurs and immediate outgroups these parasagittal metapodials have nearly equal shaft widths. A slender metatarsal 4 also occurs in noasaurids (Carrano *et al.*, 2002) and *Deltadromeus* (Sereno *et al.*, 1996). The remaining features listed, an elongate and transversely compressed ungual on manual digit I and a distal fibular shaft "reduced to a thin splint," are not autapomorphies.

Choiniere *et al.* (2012) revised the diagnosis for *Nqwebasaurus thwazi,* adding to that of the initial diagnosis. One of the additional features, a crest on the distal shaft of metacarpal 1, is unusual and diagnostic. The others, however, do not appear to stand as autapomorphies. The absence of serrations, the conical form of the teeth, and the open alveolar trough for tooth roots, for example, are common to several ornithomimosaurs and alvarezsauroids, as coded in their associated data matrix and as previously described (Sereno, 2001).

The large dataset Choiniere *et al.* (2012) used to determine the phylogenetic position of *Nqwebasaurus* resolves many additional autapomorphies for *Nqwebasaurus thwazi*, 12 of which are unambiguous. None, however, are cited in their revised diagnosis for *Nqwebasaurus thwazi*. The ovoid fossa on the ascending process of the astragalus, for example, is described as occurring elsewhere only among alvarezsauroids (Choiniere *et al.*, 2012: Tab.11, character 536) and is resolved as an autapomorphy for *Nqwebasaurus thwazi*. Nevertheless, it has a wider distribution within Ornithomimosauria and was first described and figured in *Gallimimus* (Osmólska *et al.*, 1972). The base of metacarpal 3 is flattened and expanded as in *Pelecanimimus* and other ornithomimosaurs and is not unusually broad; disarticulation of the right metacarpals may have led to the impression that the base of metacarpal 3 is broader in *Nqwebasaurus.* Other autapomorphies in this dataset for *Nqwebasaurus thwazi* may constitute unintentional coding errors; manual digit III is not longer than digit II (character 413), metacarpals 1 and 2 do not contact each other only at their proximal ends (character 394), and a femoral trochanteric crest (character 493) is not present (de Klerk *et al.*, 2000). The procumbent orientation of the preserved maxillary teeth, another resolved autapomorphy (character 228), is very likely an artifact of preservation. Unlike other theropods with procumbent crowns, the preserved teeth are far from the anterior end of the snout and do not get larger anteriorly.

Previously unrecognized diagnostic features of *Nqwebasaurus thwazi* include the beveled edge on the orbital margin of the frontal (described as a "groove" by Choiniere *et al.*, 2012: Tab. 6). Although some form of ornamentation of the orbital margin occurs elsewhere among ornithomimosaurs and more distant theropods (Longrich, 2008), the smooth, twisted form of this beveled edge appears to be diagnostic (Figs. 10, 11). The unguals of manual digits II and III, in addition, are unusually long. The ungual of manual digit III, for example, is more than twice the length of the penultimate phalanx (Tab. 1). This is a relatively longer proportion than in any other ornithomimosaur or immediate outgroup. The revised diagnosis given above is based on the foregoing comments.

DESCRIPTION

Additional details of the cranium and postcranial skeleton are described below along with measurements (Tab. 4) as a supplement to the descriptive accounts of de Klerk *et al.* (2000) and Choiniere *et al.* (2012).

Cranium (Figs. 11, 12, Tab. 4)

Portions of the skull roof and braincase are preserved. The frontal and maxilla suggest that the skull in *Nqwebasaurus* had a more primitive shape and structure than in skulls known among Early Cretaceous ornithomimosaurs, namely *Pelecanimimus* (Perez-Moreno *et al.*, 1994), *Shenzhousaurus* (Ji *et al.*, 2003) and *Harpymimus* (Kobayashi and Barsbold, 2005b). In these Early Cretaceous ornithomimosaurs, the frontal has a subtriangular shape, is more

strongly arched anteroposteriorly, and has clear demarcation of the supratemporal fossa (Fig. 12.3). The frontal forms only the posterior one half of the dorsal orbital margin, the remainder formed by an enlarged prefrontal. The frontal, in addition, is only about one half the length of the maxilla, which forms the sidewall of a long, low snout.

In *Nqwebasaurus*, in contrast, the paired frontals are hourglass-shaped, form most of the dorsal orbital margin, and have no clearly demarcated arcuate rim for the supratemporal fossa, and are approximately the same

Figure 11. ***Nqwebasaurus thwazi***, **AM** 6040. Right and left frontals and posterior portion of the left prefrontal in dorsal view. Abbreviations: **an,** articular contact for nasal; **aprf,** articular contact for prefrontal; **bs,** beveled surface; **f,** frontal; **l,** lacrimal; **pr,** process; **prf,** prefrontal; **scp,** sclerotic plate. Scale bar= 1 cm.

Table 4 – Measurements of the holotype skull bones and postcranial skeleton of **Nqwebasaurus thwazi** *(AM 6040). Length measurements of manual and pedal bones are functional, from the depth of the articular socket to the distal extremity, rather than maximum length (measuring to the extremity of the flexor surface). Measurements in mm.*

Bone	*Measurement*	*(mm)*
Cranium		
Maxilla (left)	*Length*	*25.0*
	Maximum depth	*7.7*
Frontal (right)	*Length*	*30.0*
	Minimum interorbital width	*4.5*
	Width at contact with prefrontal	*6.2*
Prefrontal	*Preserved length*	*7.0*
Sclerotic plate 1	*Length*	*3.0*
	Width	*4.5*
Sclerotic plate 2	*Length*	*2.5*
	Width	*5.0*
Axial skeleton		
Cervical 5	*Centrum length*	*(14)*
Cervical 6	*Centrum length*	*14.5*
Cervical 7	*Centrum length*	*(15)*
Cervical 8	*Centrum length*	*(16)*
Cervical 9	*Centrum length*	*14.7*
Cervical 10	*Centrum length*	*11.3*
Dorsal 1	*Centrum length*	*9.6*
Anterior dorsal	*Centrum length*	*10.0*
	Centrum diameter	*4.0*
Mid dorsal	*Centrum length*	*15.5*
	Centrum diameter	*5.0*
Chevron (anterior)	*Length*	*15.9*
	Mid shaft, anteroposterior width	*2.0*
Gastralia	*Width range*	*0.5-0.7*
Pectoral girdle		
Scapula (right)	*Length*	*64.3*
	Acromion, proximodistal width	*7.2*
	Blade, minimum neck width	*5.9*
	Blade, distal width	*13.8*
Coracoid (right)	*Dorsoventral height*	*(28)*
	Anteroposterior width	*(18)*
Radius (right)	*Length*	*43.2*
Metacarpal 1 (right)	*Length*	*15.5*
Metacarpal 1 (left)	*Length*	*(15.9)*
Metacarpal 2 (right)	*Length*	*24.0*
Metacarpal 2 (left)	*Length*	*25.7*
Metacarpal 3 (right)	*Length*	*19.0*
Metacarpal 3 (left)	*Length*	*20.0*
Phalanx I-1 (left)	*Length*	*23.0*
Ungual I-2 (left)	*Length*	*22.2*
Phalanx II-1 (left)	*Length*	*11.8*
Phalanx II-2 (left)	*Length*	*13.8*
Ungual II-3 (left)	*Length*	*17.6*
Phalanx III-1 (left)	*Length*	*8.5*
Phalanx III-2 (left)	*Length*	*6.5*
Phalanx III-3 (left)	*Length*	*8.0*
Ungual III-4 (right)	*Length*	*18.5*

Table 4 – Continuation.

Bone	Measurement	(mm)
Pelvic girdle		
Pubis	Shaft proximal to apron, transverse width	4.5
	Apron, proximal width	14.1
	Foot, distal width	6.7
	Foot, anteroposterior length	17.5
Forelimb		
Humerus	Length (right)	(58.5)
	Length (left)	(59.1)
	Head (left), transverse width	5.2
	Head (left), anteroposterior width	3.1
	Deltopectoral crest (left), length	18.3
	Distal condyles (right), transverse width	9.0
Ulna (right)	Length	44.0
Hind limb		
Tibia (right)	Length	140.2
	Proximal end, anteroposterior length	25.0
	Mid shaft, transverse width	9.4
	Mid shaft, anteroposterior width	6.9
	Distal end, transverse width	22.0
Fibula (right)	Proximal end, anteroposterior length	13.8
	Mid shaft, maximum width	2.1
Astragalus (right)	Articular surface, transverse width	15.5
	Ascending process, height	14.5
Calcaneum (right)	Articular surface, transverse width	3.1
Metatarsal 1 (right)	Length	12.8
Metatarsal 2 (right)	Length	65.3[1]
	Proximal end, transverse width	6.3
	Mid shaft, transverse width	4.0
Metatarsal 3 (right)	Length	72.8[1]
	Proximal end, transverse width	3.8
	Mid shaft, transverse width	4.4
Metatarsal 4 (right)	Length	66.0[1]
	Proximal end, transverse width	4.2
	Mid shaft, transverse width	2.0
Phalanx I-1 (right)	Length	14.8
Ungual I-2 (right)	Length	9.7
Phalanx II-1 (right)	Length	20.0
Phalanx II-2 (left)	Length	12.0
Ungual II-3 (left)	Length	16.4
Phalanx III-1 (right)	Length	22.0
Phalanx III-2 (left)	Length	19.1
Phalanx III-3 (left)	Length	12.2
Ungual III-4 (left)	Length	17.4
Phalanx IV-1 (right)	Length	10.9
Phalanx IV-2 (right)	Length	6.1
Phalanx IV-3 (right)	Length	4.4
Ungual IV-5 (right)	Length	(13.0)[2]

[1]*Shortened by 1.0 mm to compensate for gap at fracture.*
[2]*Preserved length is 8.5 mm.*

length as the maxilla (Fig. 11, 12.1–2; Tab. 4). The snout, thus, would have been proportionately shorter in *Nqwebasaurus*, which would have had a skull length of approximately 90 mm (based on maxilla and frontal lengths; Tab. 4). Although shorter snout proportions may be attributable in part, to the immaturity of the holotypic specimen of *Nqwebasaurus*, longer snout proportions are present in all but the most immature specimens of *Sinornithomimus* (*e.g.*, LH PV6; Varricchio *et al.*, 2008: fig. 3B).

Frontal (Figs. 11, 12.1–2). The frontal is well preserved on both sides and is approximately 30 mm in length (Tab. 4). The initial length measurement given for the right frontal (39 mm; de Klerk *et al.*, 2000: p. 325) included portions of the fragmented right parietal. The anterior end is V-shaped, the prefrontal suture laterally and an edge overlapped by the nasal medially (Fig. 11). In ornithomimosaurs and theropods generally, nasals taper to their posterior extremity away from the midline, and so a W-shaped prefrontal-nasal suture with the frontal is most likely in *Nqwebasaurus* (Fig. 12.1). The mid section of the frontal over the orbit narrows in width from 6.2 mm anteriorly to 4.5 mm, before expanding to twice that width at its posterior extremity (Fig. 11, 12.2; Tab. 4). The resulting hourglass shape of paired frontals in dorsal view is primitive; in other ornithomimids such as *Pelecanimimus* (Perez-Moreno *et al.*, 1994), *Shenzhousaurus* (Ji *et al.*, 2003), *Harpymimus* (Kobayashi and Barsbold, 2005b) and *Sinornithomimus* (Kobayashi and Lü, 2003), the frontals are subtriangular, narrowing in width anteriorly along their entire length and form only the posterior one half of the dorsal orbital margin. The prefrontal is expanded as a roofing element in its place and forms an equal amount of the orbital rim (Fig. 12.3).

The orbital margin is noteworthy for a characteristic non-articular, beveled edge. Starting at mid orbit and passing posteriorly, the beveled edge turns from a near vertical inclination to one facing dorsolaterally (Fig. 12.1). The beveled surface, likewise, becomes broader posteriorly and changes from being gently dorsoventrally concave to flat. It tapers to a point posteriorly near a rounded process that projects from the orbital rim. Most of the features of this beveled surface are preserved on both sides, which appears to be diagnostic for *Nqwebasaurus thwazi*. The orbital rim in ornithomimids (Longrich, 2008) and other basal coelurosaurs (*Compsognathus*; Ostrom, 1978) is modified with grooves or textures, although none have the precise form described here (*contra* Choiniere *et al.*, 2012: p. 6)

The frontal is very gently arched anteroposteriorly along its length. Unlike other ornithomimosaurs, the supratemporal fossa is poorly demarcated and limited to the posterior edge of the bone. A subtle downward curve of the posterolateral extremity of the frontal is the only contribution of the frontal to the supratemporal fossa, which would have been bordered primarily by the parietal and postorbital. This suggests that the adductor musculature was not as well developed in *Nqwebasaurus*, despite evidence it had shifted to a herbivorous or granivorous diet (reduced maxillary dentition, presence of gastroliths). The geometry of the adductor fossa in other ornithomimosaurs, in addition, is canted and the occiput and braincase rotated under the posterior skull roof. As a result, the jaw joint in subadult and adult skulls of other ornithomimosaurs is positioned ventral, rather than posterior, to the orbit (*e.g.*, *Gallimimus*; Osmólska *et al.*, 1972). Preservational factors preclude definitive determination of the condition in the earliest skulls known among other ornithomimosaurs, namely *Pelecanimimus* (Perez-Moreno *et al.*, 1994), *Shenzhousaurus* (Ji *et al.*, 2003) and *Harpymimus* (Kobayashi and Barsbold, 2005b). The anteriorly rotated jaw joint does not appear to characterize alvaezsaurids (*Shuvuuia*; Sereno, 2001: fig. 12), despite other skull and dental similarities between alvarezsaurids and ornithomimosaurs.

Prefrontal (Figs. 11, 12.1–2). Only the posterior ramus of the left prefrontal is preserved, which is lifted slightly from its natural articulation with the left frontal (Fig. 12.1). On the right side of the skull, the articular facet for the posterior tip of the prefrontal is fully exposed along the orbital margin of the frontal (Fig. 11). The posterior ramus of the prefrontal overlaps the frontal, their suture passing posterolaterally from the nasal embayment to the orbital margin. The slender posterior tip of the prefrontal curls around the orbital rim of the frontal, terminating on its ventrolateral aspect (Fig. 12.1). In other ornithomimosaurs, the prefrontal extends farther posteriorly on the skull roof to at least the mid point of the orbital rim (*Harpymimus*; Kobayashi and Barsbold, 2005b; Fig. 12.3).

Choiniere *et al.* (2012: p. 5) remarked that the prefrontal in *Nqwebasaurus* is "relatively small compared to the hypertrophied prefrontal in all other ornithomimosaurs", although

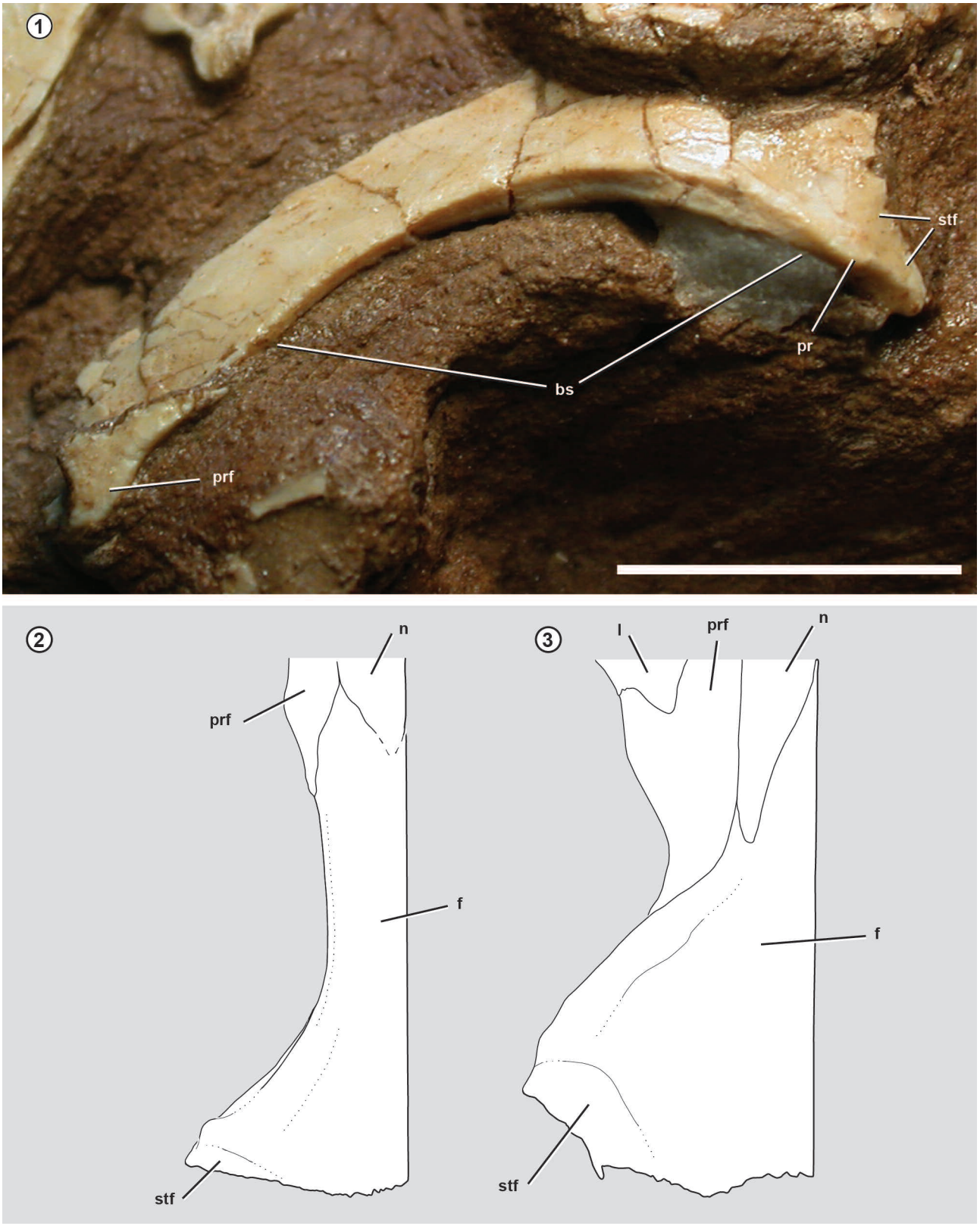

Figure 12. 1–3, ***Nqwebasaurus thwazi*****, AM** 6040. Left frontal and posterior portion of the left prefrontal; **1,** dorsolateral view; **2,** reconstruction of middle section of the dorsal skull roof. ***Struthiomimus*** sp., **TMP** 1990.26.1; **3,** drawing of middle section of the dorsal skull roof (modified from Longrich, 2008). Abbreviations: **bs,** beveled surface; **f,** frontal; **l,** lacrimal; **n,** nasal; **pr,** process; **prf,** prefrontal; **stf,** supratemporal fossa. Scale bar= 1 cm.

its relative size cannot be determined as most of the bone is broken away. It is clear, nevertheless, that the prefrontal in *Nqwebasaurus* does not contribute nearly as significantly to the orbital margin or roof as it does in other ornithomimosaurs and in alvarezsaurids (*Shuvuuia*; Sereno, 2001: fig.12). In other ornithomimosaurs and the alvarezsaurid *Shuvuuia*, the prefrontal is not only a major roofing element over the orbit but also has a broad medial ramus within the orbit (Sereno, 2001). The medial portion of the prefrontal, however, is not preserved in *Nqwebasaurus*. The unusual expanded condition of the prefrontal in other ornithomimosaurs and alvarezsaurids, in sum, may have arisen independently, given evidence from *Nqwebasaurus*.

Sclerotic plates (Fig. 11). Five sclerotic plates are preserved in the right orbit and form a portion of the right sclerotic ring. Positive plates at either end of the partial ring are fully exposed for measurement (Tab. 4).

Axial skeleton (Figs. 13–15, 16.1, Tab. 4)

Only cervical and dorsal vertebrae are preserved, the latter as disarticulated centra and neural arches. No caudal vertebrae are preserved (*contra* de Klerk *et al.*, 2000, p. 325), despite the presence of one anterior chevron. There is no evidence of ossified sternal plates as occurs in *Pelecanimimus* (Perez-Moreno *et al.*, 1994), despite preservation of both pectoral girdles and forelimbs in articulation near their natural positions (de Klerk *et al.*, 2000). A number of slender gastralia are also preserved.

One series of articulated vertebrae is present on the main block preserving the remains of *Nqwebasaurus*. De Klerk *et al.* (2000: p. 325) identified these vertebrae as "postaxial cervical vertebrae". Choiniere *et al.* (2012: p. 7) identified them more specifically as "cervical vertebrae 3–7", although they did not present supporting positional evidence. There are seven and one half vertebrae preserved in articulation, the most distal of the series represented only by the anterior one half of the centrum. The centrum length of the vertebra in advance of this partial centrum is short, has a strong hypapophysis, and is here identified as D1 (Tab. 4). Its centrum length is approximately two-thirds that of the more proximal vertebrae in the series, here interpreted as mid cervical vertebrae. It is highly unlikely that centrum length would shorten dramatically in mid cervical vertebrae, as would be the case following the identification given by Choiniere *et al.* (2012). The six complete vertebrae in the series preceding D1, thus, are most likely C10 through C5, as 10 cervicals appear to be the ususal number of cervical vertebrae in ornithomimosaurs (Osmólska *et al.*, 1972; Kobayashi and Lü, 2003).

Cervical vertebrae (Figs. 11, 12.1–2). C5-7 are the best preserved and exposed cervical vertebrae. The centrum of C5 is slightly shorter than that of C8, which is estimated to be the longest of the series (Tab. 4). In lateral view, the amphicoelous anterior and posterior faces are set at an angle to the ventral margin, resulting in a trapezoid-shaped centrum (Fig. 13.4). The ventral is concave along the anterior one half and convex along the posterior one half. The posterior convexity is accentuated by parasagittal flanges that extend ventrally from the centrum. Both centrum shape and zygapophyseal orientation suggest elevation within the neck from posterior to mid cervical verebrae.

The parapophysis is a prominent subcylindrical process located near the diapophysis, between which lies an oval pleurocoel (13.2, 13.4). Choiniere (2012) identified this invagination as a "fossa", although its position between the para- and diapophyses strongly suggests it is a pleurocel. More posteriorly on the lateral aspect of the vertebra, two open fossae are present on either side of the posterior centrodiapophyseal lamina. These can be identified dorsally and ventrally as the posterior centrodiapophyseal and centrodiapophyseal fossae (Wilson *et al.*, 2011). These cervical features distinguish *Nqwebasaurus* from those of ornithomimids from the Lower Cretaceous of western Europe, which have spool-shaped centra, show little elevation from post- to prezygapophyses, and have a pair of small anterior and posterior pleurocoels (Allain *et al.*, 2014).

The neural arch has a low, subrectangular neural spine and a broad, ventrolaterally deflected transverse process (Fig. 13.3). The diapophysis is located within the anterior one half of the centrum posterodorsal to, but not far from, the projecting, cylindrical parapophysis. The transverse process is connected to pre- and postzygapophyses by thin pre- and postzygodiapophyseal laminae (Wilson, 1999) that overhang the side of the centrum (Fig. 13.2, 13.4). A less prominent lamina (posterior centrodiapophyseal lamina) extends from the transverse process to the centrum.

The prezygapophysis is positioned far from the midline, projects anterior to the centrum face and has a strongly

anteroposteriorly convex articular surface (Fig. 13.3). These features are shared with some ornithomimosaurs (Osmólska *et al.*, 1972; Kobayashi and Lü, 2003) but are absent in Early Cretaceous ornithomimosaurs from western Europe (Allain *et al.*, 2014). In mid cervical vertebrae, the curved surface of the prezygapophysis can be deflected ventrally as much as 45° away from the plane of the articular surface of the postzygapophysis. The discordant size of pre- and postzy-

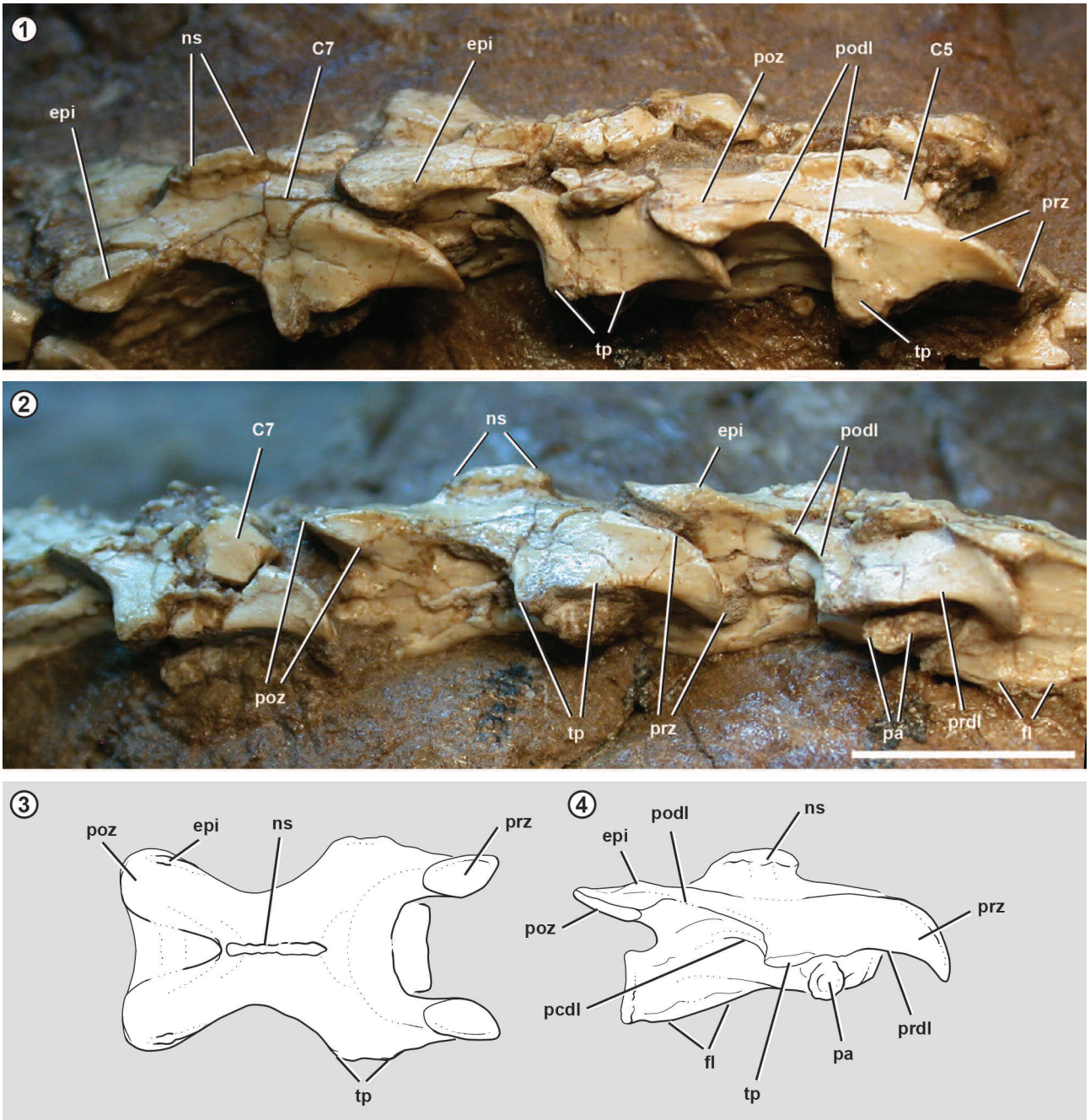

Figure 13. 1–4, ***Nqwebasaurus thwazi*****, AM** 6040. Mid cervical vertebrae; **1,** C5-7 in dorsolateral view; **2,** C5-7 in right lateral view; **3,** reconstruction of C6 in right lateral view; **4,** reconstruction of C6 in dorsal view. Abbreviations: **C5, 7,** cervical vertebra 5, 7; **epi,** epipophysis; **fl,** flange; **ns,** neural spine; **pa,** parapophysis; **pcdl,** posterior centrodiapophyseal lamina; **podl,** postzygodiapophyseal lamina; **poz,** postzygapophysis; **prdl,** prezygodiapophyseal lamina; **prz,** prezygapophysis; **tp,** transverse process. Scale bars= 5 mm in 1, and 5 mm in 2 and 3.

gapophyses is striking. In lateral view, the prezygapohpyses of mid cervical vertebrae are nearly twice as long antero-posteriorly as their opposing postzygapophyses, which resembles the condition in *Sinornithomimus* (Kobayashi and Lü, 2003). The prezygadiapohpyseal lamina spans from the prezygapophysis to the leading edge of the transverse process.

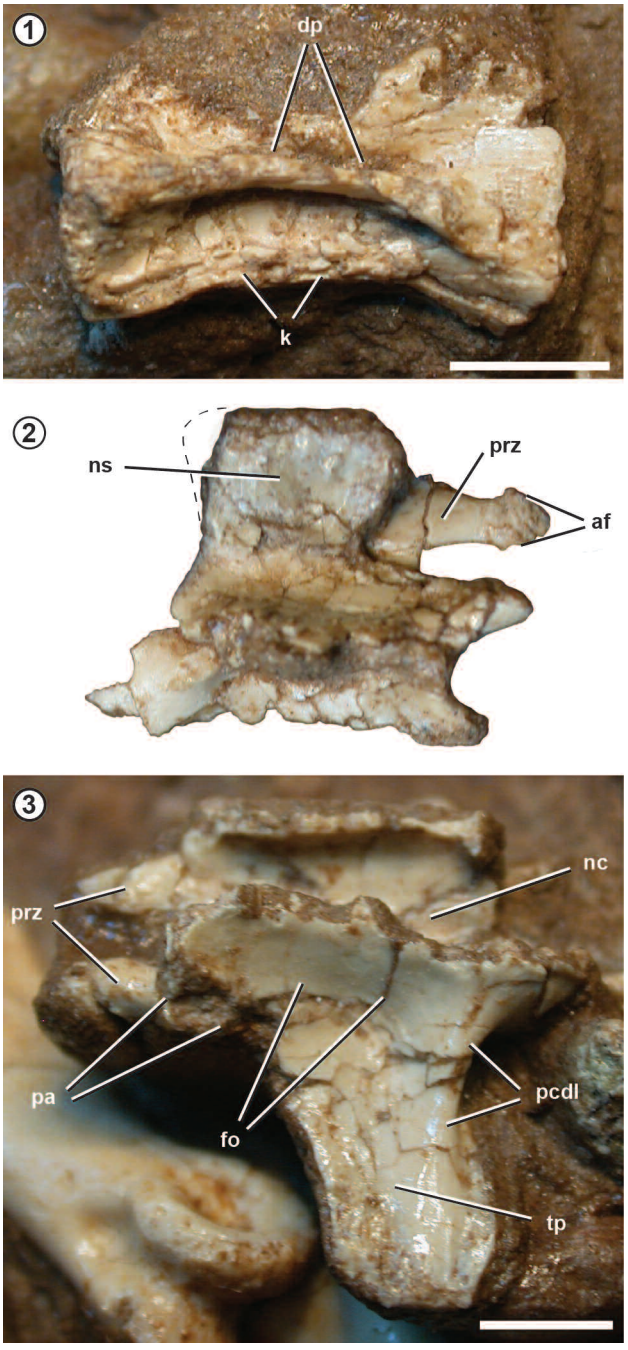

Figure 14. 1–3, ***Nqwebasaurus thwazi***, **AM** 6040. Dorsal vertebrae; **1,** mid dorsal centrum in right lateral view; **2,** mid dorsal neural arch in dorsolateral view; **3,** mid dorsal neural arch in ventrolateral view. Abbreviations: **af,** articular facet; **dp,** depresssion; **fo,** fossa; **k,** keel; **nc,** neural canal; **ns,** neural spine; **pa,** parapophysis; **pcdl,** posterior centrodiapophyseal lamina; **prz,** prezygapophysis; **tp,** transverse process. Scale bar= 1 cm.

The postzygapophyses are transversely broad and gently transversly concave, as seen on the fully exposed postzygapophysis of C7 (Fig. 13). They are connected across the midline by a broad lamina (Fig. 13.3). Epipophyses, which are present on all preserved cervical vertebrae (*contra* de Klerk *et al.*, 2000; p. 325), are displaced to the lateral side of the postzygapophysis and developed as low crests. The neural arches of posterior and mid cervical vertebrae, thus, are easy to distinguish from those of the Early Cretaceous ornithomimosaurs from western Europe, which have shorter prezygapophyses that end flush with the centrum, relatively flat and subequal pre-and postzygapophyseal articular surfaces, and narrow postzygapophyses with centered epipophyseal crests (Allain *et al.*, 2014).

Dorsal vertebrae (Fig. 14). In addition to the partial centrum of D1 located at the posterior end of the cervical series, two dorsal centra and two dorsal neural arches are preserved on the block. All of these disarticulated elements come from anterior or mid dorsal vertebrae. An anterior dorsal centrum has amphicoelous articular faces, a bulbous parapophysis on the anterodorsal edge of the centrum, pendant subrectangular hypapophysis, and pinched sides with a strong ventral keel extending the length of the centrum (Choiniere *et al.*, 2012: fig. 10; Tab. 4, anterior dorsal). There is no development of an invaginated pleurocoel, although there appears to be a slit-shaped invagination into the centrum from the neural canal (Choiniere *et al.*, 2012: fig. 10A).

A longer mid dorsal centrum also has shallow amphicoelous articular faces, its length approximately three times the diameter of either centrum face (Fig. 14.1; Tab. 4, mid dorsal). The ventral margin of the centrum is concave in lateral view, its body strongly pinched to form a ventral keel. An arched ridge runs the length of the centrum above its pinched sides. Above the ridge in the center of the centrum lies a slit-shaped depression. There is no development of an invaginated pleurocoel.

A dorsal neural arch has a hatchet-shaped neural spine that is slightly longer than deep (Fig. 14.2). The prezygapophyses have relatively small, subtriangular articular surfaces that that angle ventromedially. The articular facet

of each prezygapophysis is slightly expanded at the end of the prezygapophyseal process, which is unusually long and gently waisted at mid length (Fig. 14.2). The prezygapophyseal facet is flat with no development of a hypantrum articulation. Although the condition is poorly reported among ornithomimosaurs, this stabilizing intervertebral articulation is not present in mid dorsal vertebrae in *Sinornithomimus* (LH PV6) and appears to be limited to the most poserior vertebrae in *Gallimimus* (Osmólska *et al.*, 1972, pl. 53, fig. 4d). The subrectangular transverse process, best preserved in ventral view of a second dorsal neural arch (Fig. 14.3), is directed laterally just above the horizontal and slightly posteriorly. A rounded posterior centrodiapophyseal lamina is present, anterior to which is a shallow fossa on the neural arch.

Chevron. One slender, transversley compressed anterior chevron is preserved, its distal end turned slightly posteriorly. This chevron closely resembles Ch2 and 3 in *Shenzhousaurus* (Ji *et al.*, 2003: fig. 8).

Gastralia (Fig. 15). Several gastralia are preserved near one another but not in articulation. Some of the shafts are truncated with perpendicular broken ends. All of the gastral elements are slender rods measuring less than 1 mm in diameter (Tab. 4). The rods are nearly uniform in diameter; none taper to splint-shaped ends, as is common along the scarf-shaped articulation between medial and lateral gastral elements in other theropods. Likewise, none have spatulate ends as occurs in the lateral gastral elements of *Shenzhosaurus* (Ji *et al.*, 2003: fig. 9) and later ornithomimosaurs (Osborn, 1917 Sternberg, 1933). Although most of the gastral elements are truncated as a result of breakage, several of the gastral elements appear to preserve slighly expanded, squared distal ends (Fig. 15). The gastralia in *Nqwebasaurus*, thus, appear to be simpler in form than in the gastral cuirass preserved in other ornithomimosaurs.

Pectoral girdle and forelimb (Figs. 16, 17, Tab. 4)

In the description below, the scapula and coracoid are oriented with the scapular blade held horizontal and the "posterior" process of the coracoid pointing ventrally. This orientation more closely approximates its orientation in life, as suggested by its position in the articulated skeleton of *Nqwebasaurus* (de Klerk *et al.*, 2000: fig. 2).

Furcula, sternal plates. There is no trace of an ossified furcula

Figure 15. ***Nqwebasaurus thwazi*****, AM** 6040. Gastralia. Arrows point to the ends to gastral elements that appear to be finished rather than broken. Scale bar= 5 mm.

or sternum, despite preservation of both pectoral girdles and forelimbs in articulation near their natural positions (de Klerk *et al.*, 2000). The lack of an ossified furcula and sternum is common among ornithomimids, as shown without any question in the mud-trapped skeletons of *Sinornithomimus* (Kobayashi and Lü, 2003; Varricchio *et al.*, 2008). Exceptional preservation in *Pelecanimumus*, however, reveals the presence of paired sternal plates, although there is no evidence of an ossified furcula (Perez-Moreno *et al.*, 1994). An ossified furcula, however, was discovered recently in a partial skeleton of the large-bodied, stout-limbed ornithomimosaur *Deinocheirus* (Lee *et al.*, 2014), although no ossified sternal plates were reported. The ossification of these elements, thus, appears to vary among ornithomimosaurs.

Scapula (Fig. 16). The scapula is more primitive in a number of features compared to other ornithomimosaurs such as *Sinornithomimus* (Kobayashi and Lü, 2003: fig. 15). In lateral view the acromion, which is best preserved on the left side, (Fig. 16.2) is subquadrate in shape (Fig. 16.3), whereas in *Sinornithomimus* it is subrectangular (*i.e.*, longer along the axis of the blade than deep). Just posterior to the glenoid is a shallow textured fossa for muscle attachment (Fig. 16.1, 16.3), as occurs in other ornithomimosaurs (Osmólska *et al.*, 1972). There is no development of a supraglenoid buttress, and the oval scapular glenoid faces anteroventrally (Fig. 16.1, 16.3). In other ornithomimosaurs, a ridge-like supraglenoid buttress is present, and the partially everted glenoid is visible in lateral view (Osmólska *et al.*, 1972; Nichols and Russell, 1985; Kobayashi and Lü, 2003). The blade is expanded distally to twice the width at the neck of the scapula (Tab. 4), and the midline axis of the blade curves slightly dorsally toward its distal end, rather than ventrally, as in many other ornithomimosaurs (Osmólska *et al.*, 1972; Kobayashi and Lü, 2003).

Coracoid (Figs. 16, 17). The coracoid is more primitive in a number of features compared to other ornithomimosaurs such as *Sinornithomimus*, *Gallimimus* or *Struthiomimus* (Osmólska *et al.*, 1972; Nichols and Russell, 1985; Kobayashi and Lü, 2003). Choiniere *et al.* (2012: Tab. 9) suggested that

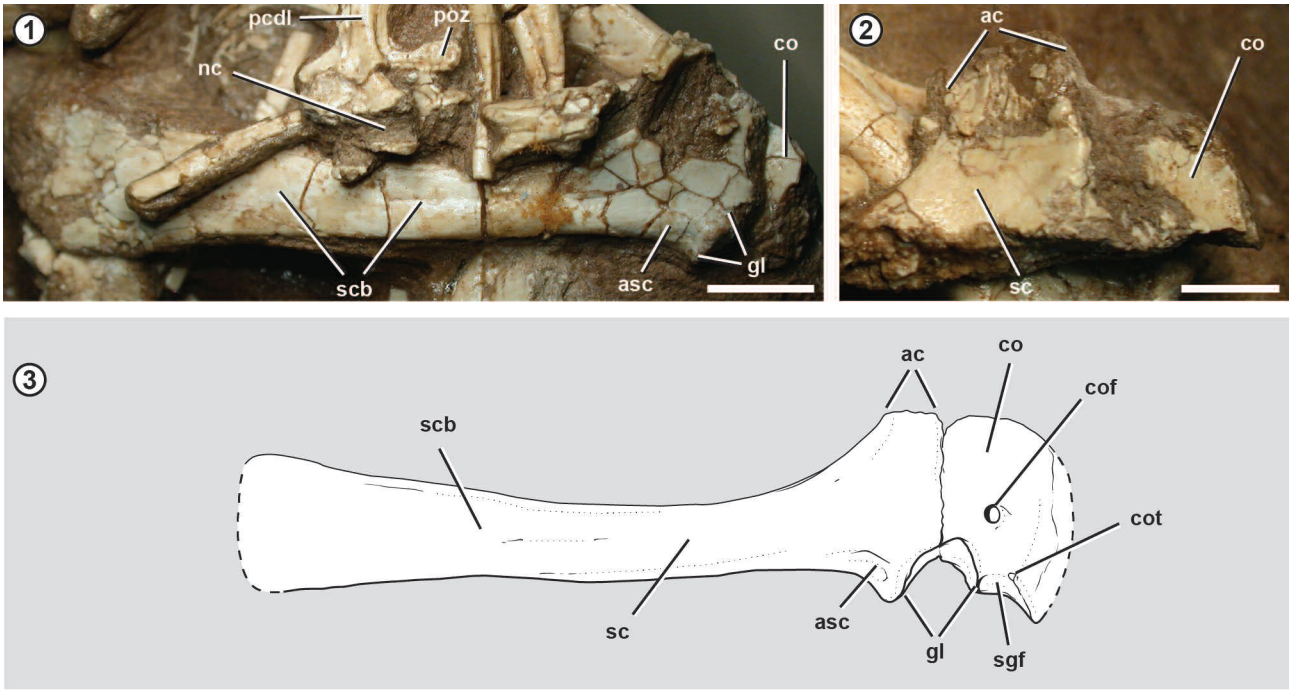

Figure 16. 1–3. ***Nqwebasaurus thwazi*****, AM** 6040. Scapula and coracoid. **1,** right scapula in lateral view; **2,** left proximal scapula and coracoid in medial view; **3,** reconstruction of right scapulocoracoid in lateral view. Abbreviations: **ac,** acromion; **asc,** attachment scar; **co,** coracoid; **cof,** coracoid foramen; **cot,** coracoid tubercle; **gl,** glenoid; **nc,** neural canal; **pcdl,** posterior centrodiapophyseal lamina; **poz,** postzygapophysis; **sc,** scapula; **scb,** scapular blade; **sgf,** subglenoid fossa. Scale bar= 1 cm in 1 and 5 mm in 2.

the coracoid has the dorsoventrally elongate proportions typical of ornithomimosaurs. The anterior edge of both coracoids, however, is incomplete (Fig. 17.1), compromising a precise assessment of its proportions. The preserved portion of the ventral (posterior) process, nonetheless, suggests that the coracoid was not as dorsoventrally elongate as in other ornithomimosaurs (Fig. 16.3). The coracoid tubercle is extended ventrally by a sharp ridge flanked by a shallow subglenoid fossa as in other ornithomimosaurs (Osmólska *et al.*, 1972; Nichols and Russell, 1985; Kobayashi and Lü, 2003), although the tubercle is less pronounced in *Nqwebasaurus* (Fig. 17). The coracoid foramen is positioned a good distance anterior to the scapular suture in lateral view and opens into a canal that probably exits medially entirely within the coracoid as in other ornithomimosaurs.

The form and position of the coracoid tubercle and subglenoid fossa are primitive. Both are positioned ventrally at the level of the ventral lip of the glenoid (Figs. 16.3, 17.1), whereas in other ornithomimosaurs they are positioned dorsally adjacent to the upper one half of the glenoid (Osmólska *et al.*, 1972; Nichols and Russell, 1985; Kobayashi and Lü, 2003). The subglenoid fossa is shallow and broadly arched in *Nqwebasaurus* (Fig. 17.1), whereas in other ornithomimosaurs the fossa is deeper and subtriangular, the ventral margin shaoed as a notch, and the fossa marked by a distinctive pit immediately ventral to the coracoid tubercle. The coracoid tubercle in other ornithoimimisaurs, in addition, is extended dorsally by a ridge, a surface that is rounded in *Nqwebasaurus* (Fig. 17.1).

Humerus, radius and ulna (Figs. 18.1–2, 19). The deltopectoral crest of the humerus is well-developed, occupying approximately one third of the proximal end (Fig. 18.1), compared to the weaker crest in other ornithomimosaurs. The oval humeral head is broader than deep unlike the posteriorly offset, subcircular humeral head in other ornithomimosaurs (Tab. 4). The humeral shaft follows a sigmoid curve, bowed posteriorly in the region of the deltopectoral crest and anteriorly near the distal condyles. This curvature of the humeral shaft is primitive. In other ornithomimosaurs such as *Sinornithomimus* and *Gallimimus* (Kobayashi and Lü, 2003; Osmólska *et al.*, 1972), the humeral shaft is bowed medially, which is most most strongly expressed in *Beishanlong* (Makovicky *et al.*, 2009). The distal end is expanded transversely from the shaft, more so than in other ornithomimosaurs (Fig. 18.2). A shallow fossa is present on the posterior aspect of the distal end to accommodate the olecranon process of the ulna. The humerus is slightly shorter than the combined length of the radius and metacarpal 3 (Tab. 4), which is very close to the proportions in *Sinornithomimus* (Kobayashi and Lü, 2003).

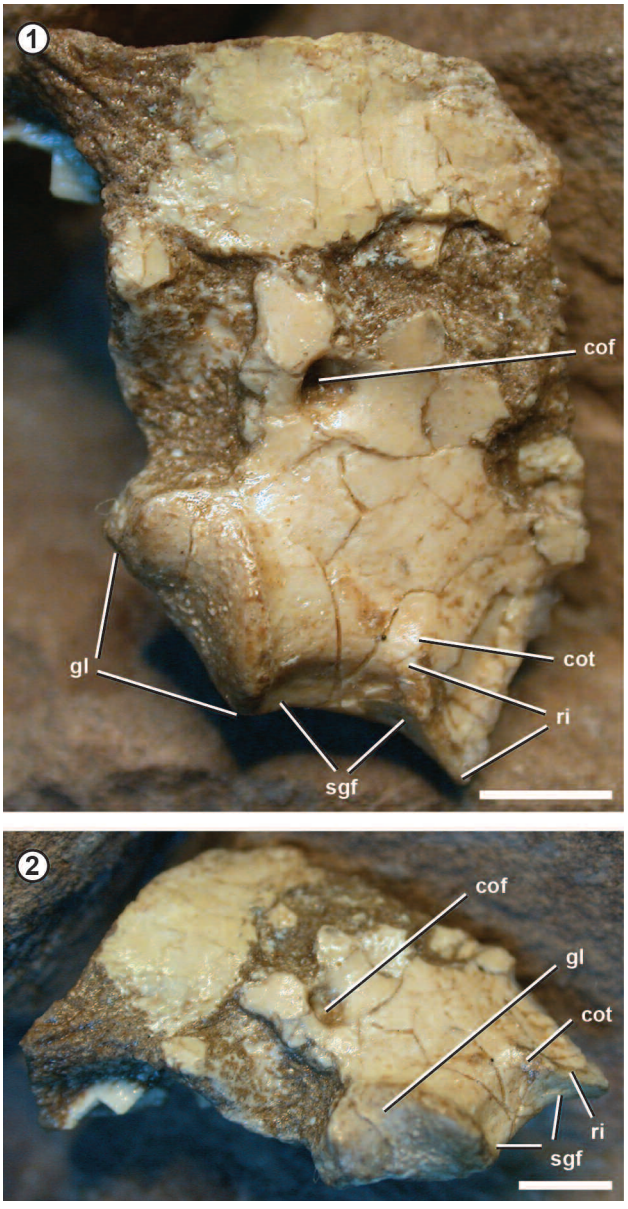

Figure 17. 1–2. ***Nqwebasaurus thwazi*****, AM** 6040. Right corocoid. **1,** right coracoid in lateral view; **2,** right coracoid in posterolateral and ventral view. Abbreviations: **cof,** coracoid foramen; **cot,** coracoid tubercle; **gl,** glenoid; **ri,** ridge; **sgf,** subglenoid fossa. Scale bar= 5 mm.

The shafts of the radius and ulna (Fig. 19), although flattend where they oppose one another, are clearly separated by an interosseous space along their lengths, unlike the apressed shafts in *Sinornithomimus* (Kobayashi and Lü, 2003) and *Struthiomimus* (Nichols and Russell, 1985). A tapering olecranon process is preserved on the right side (Fig. 18.1), which is better developed than in *Sinornithomimus* (Kobayashi and Lü, 2003) and *Struthiomimus* (Nichols and Russell, 1985). The structure of the forearm, thus, is not as derived as in other ornithomimosaurs.

Carpus (Fig. 13). Two carpals are preserved in *Nqwebasaurus* on both sides. The medial element, reasonably identified as the semilunate carpal, is larger, flatter, and positioned over metacarpals 1 and 2 on the right side (Fig. 18.1). On the left side, the semilunate carpal is dislodged to the lateral side of the base of metacarpal 1, exposing its concave proximal articular surface (Fig. 19). The smaller oval carpal may represent the radiale. On the right side it may be near its natural position at the distal end of the radius (Fig. 18.1). On the left side, the radiale is dislodged to the side of the base of metacarpal 2, exposing a flat (possibly distal) articular surface (Fig. 19). In other ornithomimosaurs, the number of carpals varies from three (*Sinornithomimus*; Kobayashi and Lü, 2003) to five (*Pelecanimimus*, *Struthiomimus*; Perez-Morenao *et al.*, 1994; Nichols and Russell, 1985). A semilunate carpal, the largest among them, is always present and positioned over metacarpals 1 and 2.

Manus (Figs. 18, 19). The manus is more primitive in a number of features compared to other ornithomimosaurs such as *Shenzhousaurus* (Ji *et al.*, 2003), *Harpymimus* (Kobayashi and Barsbold, 2005b), *Pelecanimimus* (Perez-Moreno *et al.*, 1994), *Sinornithomimus* (Kobayashi and Lü, 2003) and *Gallimimus* (Osmólska *et al.*, 1972). These primitive features are manifest in the length and form of the metacarpals, nonungual phalanges and unguals.

The metacarpals show primitive disparity in length (Fig. 18.3). Metacarpals 1 and 3 are 65% and 79% the length of metacarpal 2, respectively. In other ornithomimosaurs, metacarapal 1 is at least 80% of metacarpal 2, which is subequal to metacarpal 3 in length. The metacarpals in *Nqwebasaurus* also have waisted shafts (Fig. 18.3), whereas in other ornithomimosaurs, the metacarpal shafts do not expand as much approaching the distal condyles.

Metacarpal 2 has divided distal condyles and a dorsal extensor depression for the proximal phalanx in dorsal view (Fig. 18.3). Metacarapal 2 in *Harpymimus* approaches this condition, although the dorsal extensor depression for the proximal phalanx is poorly developed (Kobayashi and Barsbold, 2005b). The condition in *Nqwebasaurus* and *Harpymimus* is indicative of substantial extension at the metacarpal-phalangeal joint. In other ornithomimosaurs, the distal condyles of metacarpal 2 are divided only in ventral view (Osmólska *et al.*, 1972; Nichols and Russell, 1985), and extension at the metacarpal-phalangeal joint is very limited (Osmólska *et al.*, 1972; Sereno, 2001).

Metacarpal 3 has a wide flange for articulation with the ventral aspect of the base of metacarpal 2. This overlap is partially preserved on the left side (Fig. 19) but fully disarticualted on the right side (Fig. 18.1). When the base of metacarpal 3 is repositioned ventral to metacarpal 2 (Fig. 18.3), the width of the metacarpus closely matches the width of the conjoined distal ends of the radius and ulna (Fig. 18.1). In other ornithomimosaurs, the metacarpus is more compact. The metacarpal shafts are more closely aligned, and the base and proximal articular surface of metacarpal 3 is less expanded, taking on a wedge, rather than flange, shape as is well shown in *Harpymimus* (Kobayashi and Barsbold, 2005b), *Shenzhousaurus* (Ji *et al.*, 2003), *Sinornithomimus* (Kobayashi and Lü, 2003), *Gallimimus* (Osmólska *et al.*, 1972) and *Struthiomimus* (Nicholls and Russell, 1985). The dorsal portion of the distal condyles of metacarpal 3 are broken away in the right manus (Fig. 18.1). In ventral view of the left manus (Fig. 19), the condyles of metacarpal 3 are well developed and separate. The proximal phalanx is extended on these condyles to a degree that may have required at least a shallow dorsal extensor depression, as is present in basal tetanurans such as *Sinraptor* (Currie and Zhao, 1993). For the time being, the reconstruction of the manus of *Nqwebasaurus* shows metacarpal 3 with a single rounded condyle in dorsal view as occurs in *Harpymimus* (Kobayashi and Barsbold, 2005b). In dorsal view of metacarpal 2 and 3, there is very little rounding of the distal condyle in other ornithomimosaurs such as *Sinornithomimus* (Kobayashi and Lü, 2003), *Gallimimus* (Osmólska *et al.*, 1972) and *Struthiomimus* (Nicholls and Russell, 1985).

Proximal phalanx I-1 has a short dorsal intercondylar process as seen in the left manus (Fig. 19). This process is

retained in other ornithoimimosaurs (Osmólska *et al.*, 1972; Sereno, 2001). Proximal phalanx II-1 also has a dorsal intercondylar process (Fig. 18.3), which is absent in *Harpymimus* (Kobayashi and Barsbold, 2005b), *Shenzhousaurus* (Ji *et al.*, 2003), *Sinornithomimus* (Kobayashi and Lü, 2003) and *Struthiomimus* (Nichols and Russell, 1985). The process is partially exposed in the left manus (Fig. 19). This process can also be inferred from the paired, deeply and completely divided distal condyles and well-developed dorsal extensor depression of the left metacarpal 2 (Fig. 18.1, 18.3). A short dorsal intercondylar process may also be present on proximal phalanx III-1 (Fig. 18.3), although this is uncertain. The dorsal edge of the base of this phalanx is broken away in the right manus (Fig. 18.1). In the left manus, this phalanx is only exposed in ventral view (Fig. 19). Although the condyles of metacarpal 3 are divided in ventral view, the presence or absence of condylar division or a dorsal extensor depression for a dorsal intercondylar process of phalanx III-1 cannot be determined.

In ventral view, all proximal phalanges have rudimentary paired flexor proceses (Fig. 19) as occurs in the manus of *Pelecanimimus* (LHo 7777; Perez-Moreno *et al.*, 1994), *Shenzhousaurus* (Ji *et al.*, 2003) and more derived ornithomimosaurs. The other non-ungual phalanges (phalanx II-2, III-2, III-3) have tongue-shaped ventral intercondylar processes (Fig. 19). These processes articulate proximally

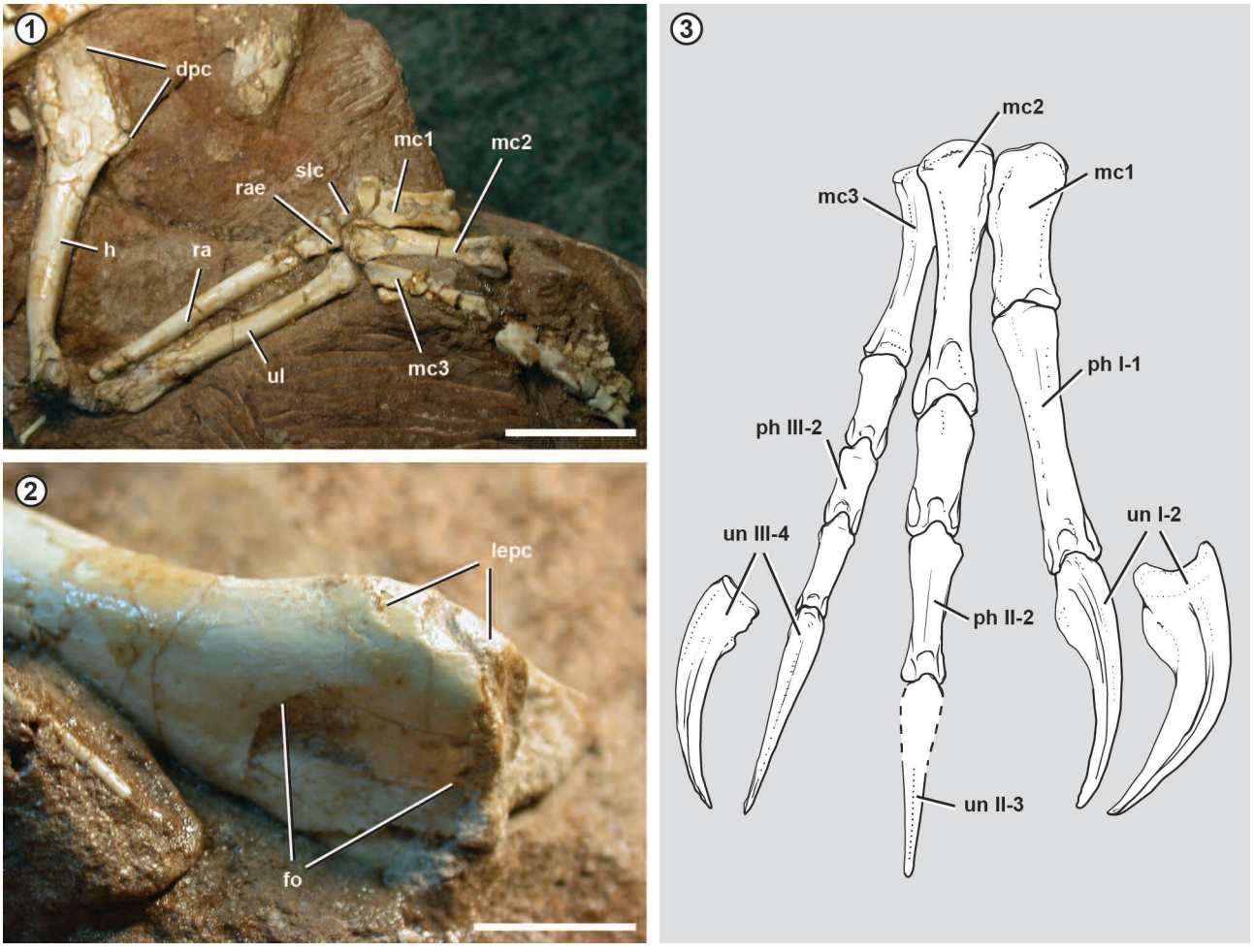

Figure 18. 1–3. ***Nqwebasaurus thwazi***, **AM** 6040. Right forelimb. **1,** right forelimb with humerus in lateral view and forearm and manus in dorsal view; **2,** distal right humerus in posterior view; **3,** reconstruction of right manus in dorsal view with lateral views of the unguals. Abbreviations: **dpc,** deltopectoral crest; **fo,** fossa; **h,** humerus; **lepc,** lateral epicondyle; **mc1–3,** metacarpal 1–3; **ph,** phalanx; **ra,** radius; **rae,** radiale; **slc,** semilunate carpal; **ul,** ulna; **un,** ungual. Scale bar= 2 cm in 1, and 5 mm in 2.

with ginglimoid distal condyles characterized by marked collateral ligament pits and a median flexor fossa. The flexor fossa accommodates the ventral intercondylar process during maximum flexion and indicates that a considerable amount of rotation was possible at these interphalangeal joints. Similar conditions appear to be present in *Shenzhousaurus* (Ji *et al.*, 2003) and *Harpymimus* (Kobayashi and Barsbold, 2005b). In more derived ornithomimosaurs such as *Sinornithomimus* (Kobayashi and Lü, 2003) and *Struthiomimus* (Nichols and Russell, 1985), the socket and condyle of these joints are closely fitted to prevent significant rotation. Broken metacarpal and non-ungual phlanageal shafts in the right manus show that all of the long bones of the manus are hollowed.

The penultimate phalanges of digits I-III in *Nqwebasaurus* are proportionately shorter than in other ornithomimosaurs. Phalanx I-1 is slightly shorter than metacarpal 2 (Tab. 4), whereas in *Harpymimus* (Kobayashi and Barsbold, 2005b) and other ornithomimosaurs, phalanx I-1 always exceeds the length of metacarpal 2. Penultimate phalanx II-2 and III-3, likewise, are relatively short, measuring only 117% the length of phalanx II-1 and 53% the length of phalanx III-1 plus III-2, respectively (Fig. 18.3, Tab. 4). In other ornithomimosaurs, phalanx II-2 is more than double the length of phalanx II-1, and phalanx III-3 always exceeds the sum of the lengths of phalanx III-1 and III-2.

The unguals on manual digits I and III the best exposed (Fig. 18.3). Ungual I-1, which is the longest and deepest of the manual unguals (Tab. 4), is the most recurved as is common among ornithomimosaurs. The large convex flexor tubercle is shifted a short distance distally from the proximal articular socket. Ungual II-3 and III-4 are less recurved and have small, distally shifted flexor tubercles (*contra* Choiniere *et al.*, 2012, who reported that flexor tuberlces are absent). The recurvature of ungual III-4 (and probabaly ungual II-3) is similar to that in *Shenzhousaurus* (Ji *et al.*, 2003) measured as follows: with the proximal articular socket oriented vertically, these manual unguals curve well below a horizontal line coincident with the ventral edge of the proximal articualar end. In most ornithomimosaurs, the unguals of manual digits II and III are considerably straighter; the distal tip is positioned close to a horizontal line drawn as described above. These straighter unguals characterize *Harpymimus* (Kobayashi and Barsbold, 2005b), *Pelecanimi-*

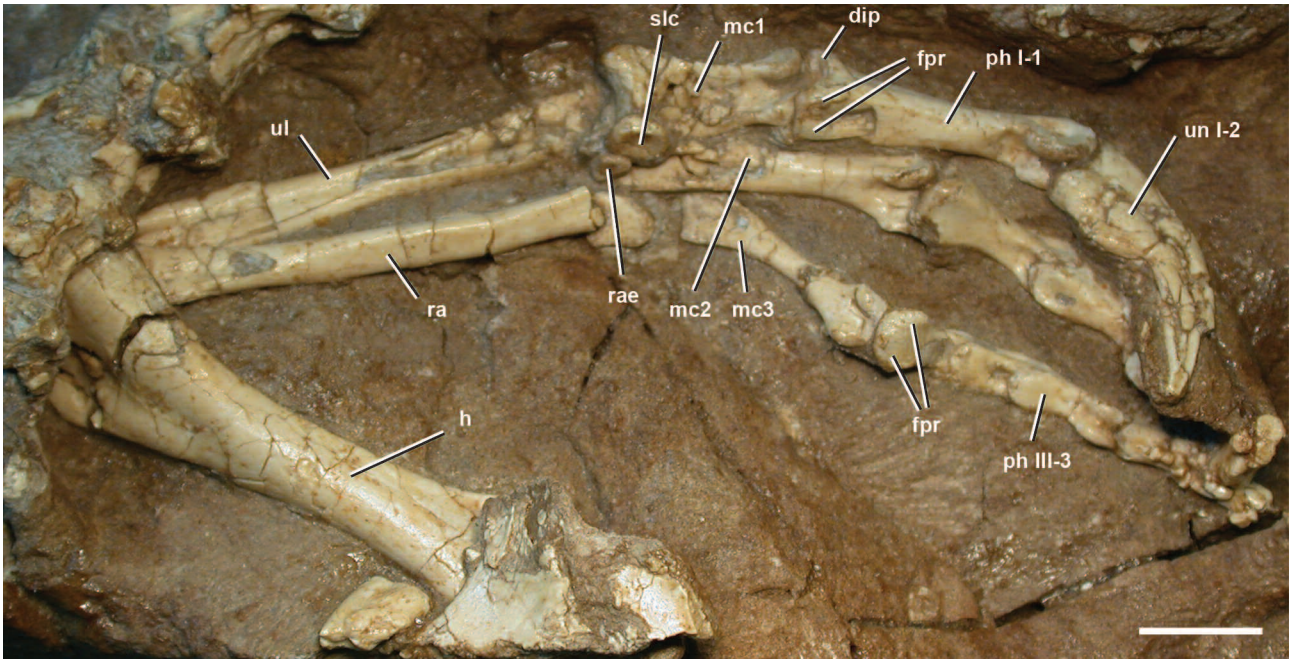

Figure 19. ***Nqwebasaurus thwazi*, AM** 6040. Left forelimb with forearm, carpus and manus in ventral view. Abbreviations: **I, III,** manual digits I, III; **dip,** dorsal intercondylar process; **fpr,** flexor process; **h,** humerus; **mc1–3,** metacarpal 1–3; **ph,** phalanx; **ra,** radius; **rae,** radiale; **slc,** semilunate carpal; **ul,** ulna; **un,** ungual. Scale bar= 1 cm.

mus (Perez-Moreno *et al.*, 1994; *contra* Choiniere *et al.*, 2012), *Sinornithomimus* (Kobayashi and Lü, 2003) and *Struthiomimus* (Nichols and Russell, 1985). In *Nqwebasaurus*, the manual unguals are also proportionatley longer than in other ornithomimosaurs compared to other elements of the manus. Manual ungual I-1 is subequal in length to phalanx I-1, whereas in other ornithomimosaurs the reverse relationship holds. Manual ungual III-4 is also longer than the preceding penultimate phalanx and nearly as long as metacarpal 3. An alternative interpretation might hold that all ornithomimosaurs have relatively large unguals compared to other manual elements but that ornithomimosaurs more derived than *Nqwebasaurus* have lengthened the metatarsals and penultimate phalanges relative to the unguals.

Pelvic girdle and hind limb (Figs. 20–24, Tab. 4)

Pubis (Fig. 20). The pubis, the only element of the pelvic girdle preserved, has relatively narrow proportions in anterior view (Fig. 20). The pubic apron tapers from a maximum transverse width of just over 14 mm proximally to approximately one half that near the foot distally (Tab. 4). These proportions are slightly longer than, but otherwise very similar to, that of the pubic apron in *Ornitholestes* (Carpenter *et al.*, 2005).

De Klerk *et al.* (2000: p. 328) remarked that the "pubic foot has a very indistinct outline; it may have been finished in cartilage in life and thus not fully preserved". This accurately describes the condition of the distal end of the pubes, the surface texture of which appears weathered. The form of the pubic foot, nevertheless, is discernible. The pubic apron can be seen extending under the proximal ends of the right tibia and fibula, with right and left sides in natural artciulation (Fig. 20). The lateral edge of the apron forms a rounded shaft, with the apron extending medially from its anterior edge as a thin sheet. The distal end of the pubes, which emerge from under the tibia and fibula, appears fused, somewhat flattened and exposed anterolateral view. The foot, which appears relatively broad transversely, has no development of an anterior projection but has a short posterior projection, as preserved in cross-section (Fig. 20). The pubic foot, thus, would appear in lateral view as to be

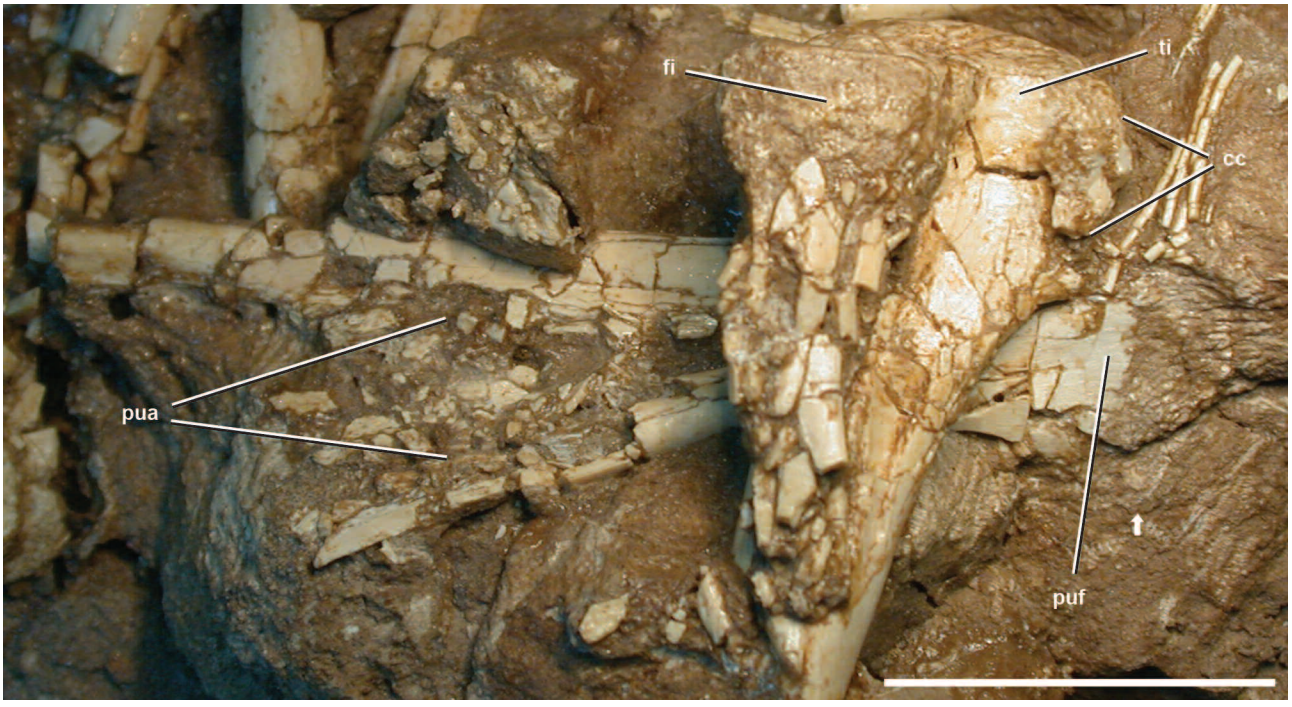

Figure 20. ***Nqwebasaurus thwazi*, AM** 6040. Proximal right tibia and fibula in lateral view and conjoined pubes in anterior view. Arrow indicates the posterior tip of the short pubic foot. Abbreviations: **cc,** cnemial crest; **fi,** fibula; **pua,** pubic apron; **puf,** pubic foot; **ti,** tibia. Scale bar= 3 cm.

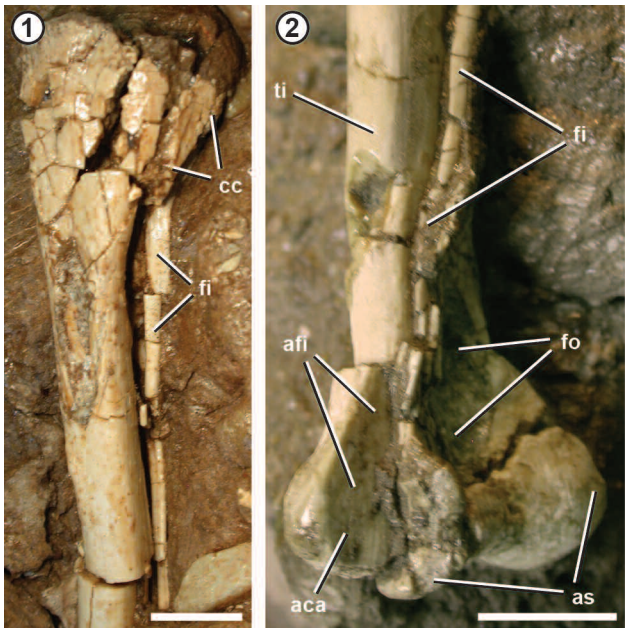

Figure 21. 1–2. ***Nqwebasaurus thwazi*****, AM** 6040. Tibia and fibula. **1,** proximal left tibia and fibula in lateral view; **2,** ditsal right tibia, fibula and astragalus in anterolateral view. Abbreviations: **aca,** articular surface for the calcaneum; **afi,** articular surface for the fibula; **as,** astragalus; **cc,** cnemial crest; **fi,** fibula; **fo,** fossa; **ti,** tibia. Scale bar= 1 cm.

club-shaped and expanded in a posterior direction only, as in the compsognathid *Scipionyx* (Dal Sasso and Maganuco, 2011). The pubic foot in the basal alvaresaurid *Patagonykus* has a similar, although more pointed, posterior process (Novas, 1997). The condition of the pubic foot in *Ornitholestes* is unknown (Carpenter *et al.*, 2005). In other ornithomimosaurs, the pubic foot has anterior and especially strong posterior projections (Osmólska *et al.*, 1972; Kobayashi and Barsbold, 2005b; Lee *et al.*, 2014). The condition of the pubic foot in *Nqwebasaurus* is comparatively primitive.

Tibia (Figs. 20, 21). Both tibiae are preserved, the right in lateral view covered proximally by the fibula and the left in medial view. In lateral view, the cnemial crest is only moderately developed, expanding a short distance from the shaft as seen on both sides (Figs. 20, 21). As in *Afromimus*, the cnemial crest is not strongly deflected laterally. As a result, the tibial incisure, or trough, between the crest and the lateral condyle is broadly open laterally. The cnemial crest, in addition, does not bulge proximally to become the most prominent aspect of the proximal end. In these regards, *Nqwebasaurus* is similar to compsogathids (Ostrom, 1978; Dal Sasso and Maganuco, 2011) and differs from other Early Cretaceous ornithomimosaurs from western Europe (Allain *et al.*, 2014) as well as many other theropods.

The distal end of the tibia is best exposed on the right side, where it is covered in part by the right astragalus (Fig. 21.2). The distal end of the fibula and calcaneum, however, have broken away, exposing the broad, flat surface of the lateral malleolus. The transverse width available for the distal end of the fibula and calcaneum is far greater than in *Sinornithomimus* (LH PV7), *Beishanlong* (Shapiro *et al.*, 2003; Makovicky *et al.*, 2009) and other ornithomimosaurs.

Fibula (Figs. 20, 21). The weathered proximal end of the fibula perserves internal cancellous internal bone, distal to which the shaft is fractured (Fig. 20). The pieces of the fractured shaft are separated by matrix, suggesting that the lateral wall was thin and enclosed an ample fibular fossa as in *Afromimus* (Fig. 6.4) and other ornithomimosaurs. The shaft of the fibula becomes quite slender more distally, as exposed on the left side distal to the cnemial crest (Fig. 21.1). The medial aspect of the fibular shaft is flattened for close approximation to the tibia. The slender distal fibula is preserved on the right side, its distalmost end broken away (Fig. 21.2). The space for the distal end of the fibula suggests that it would have expanded in transverse width as in *Afromimus* (Fig. 7.1).

Pes (Figs. 22–24). The pes is well known from partial, articulated right and left pedes, with metatarsal 5 the only bone not visible. Pedal digit I is long enough to have contacted the substrate, a condition more primitive than in *Sinornithomimus* (LH PV7), which retains a vestigial pedal digit I. In *Nqwebasaurus* pedal digit III is considerably longer than pedal digits II and IV (Fig. 22.2), a stronger digital disparity than in *Sinornithomimus* (LH PV7; Kobayashi and Lü, 2003) and more equivalent to the condition in *Gallimimus* (Osmólska *et al.*, 1972).

Pedal digit I is preserved in natural articulation on the posteromedial aspect of the distal shaft of metatarsal 2 of the right pes (Fig. 22.1). Metatarsal 1 has a beveled, concave flange-shaped base for articulation with the posterolateral aspect of the shaft of metatarsal 2 and distal condyles that are weakly divided. Proximal phalanx I-1 does not have a dorsal intercondylar process. It extends past the distal condyle of metatarsal 2, which would allow the ungual of digit I to come into contact with the substrate. Ungual I-2 is directed posteriorly, as is the ungual in the

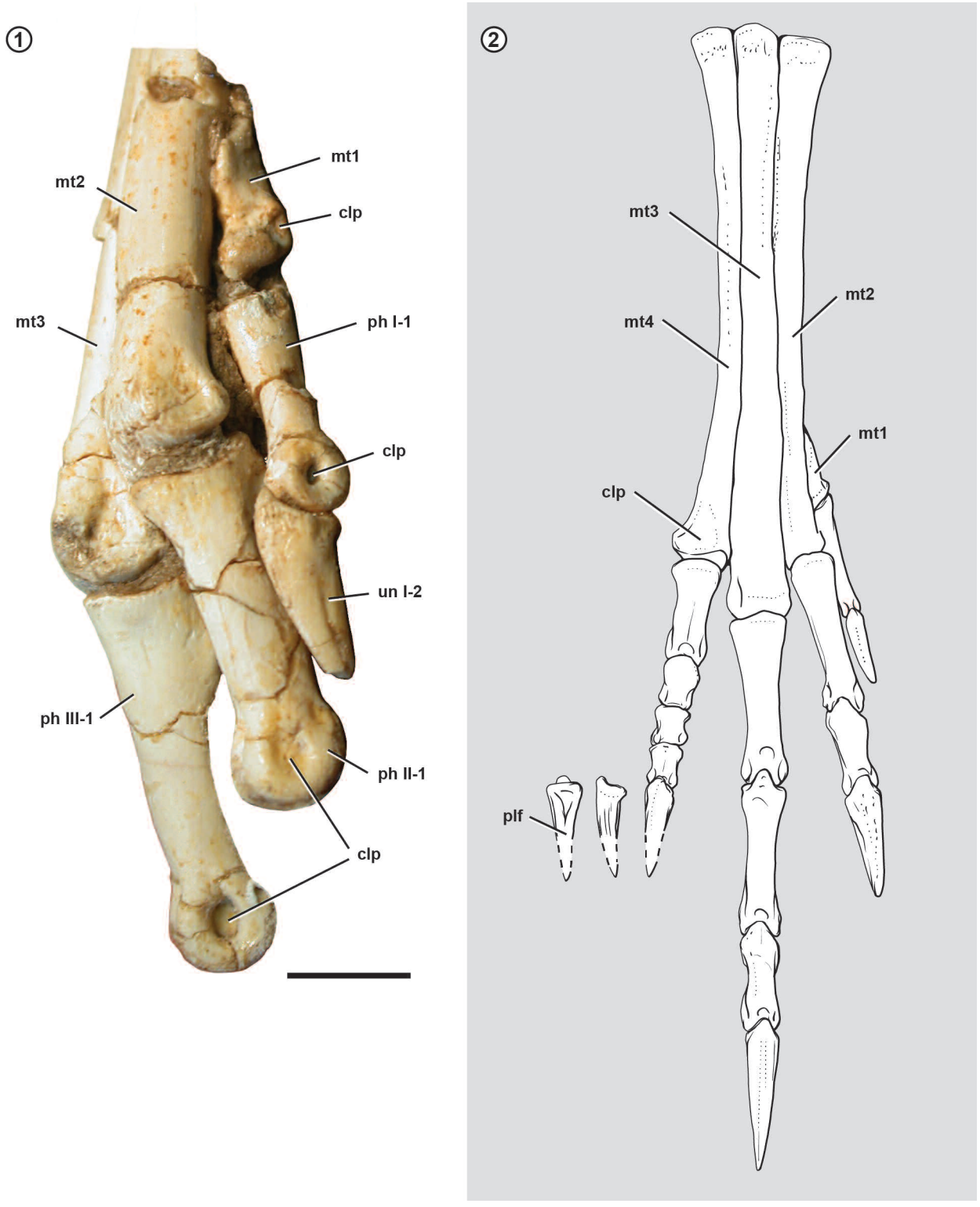

Figure 22. 1–2. ***Nqwebasaurus thwazi***, **AM** 6040. Right pes. **1,** right pes showing natural articulation of digit I alongside digit II in dorsomedial view. **2,** reconstruction of right pes in dorsal view with lateral and ventral views of the ungual of digit IV. Abbreviations: **I-III,** pedal digits I-III; **clp,** collateral ligament pit; **mt1-4,** metatarsal 1-4; **ph,** phalanx; **plf,** platform; **un,** ungual. Scale bar= 1 cm.

vestigial pedal digit I preserved in *Sinornithomimus* (LH PV7).

The metatarsal bundle, composed of metatarsals 2–4, is well exposed on the rigit side (Fig. 22). As is common, metatarsal 3 is longest, and metatarsal 4 is slightly longer than metatarsal 2 (Tab. 4). The semicircular proximal articular surface of metatarsal 2 and the subcircular proximal articular surface of metatarsal 4 comprise the largest and smallest articular surfaces for the distal tarsals, repsectively (Fig. 23.1). The proximal articular surface of metatarsal 3 is subrectangular, tapering slightly in width posteriorly and with concave medial and lateral edges. The proximal articular surface of metatarsal 3, thus, does not resemble the more derived condition in *Harpymimus* (Kobayashi and Barsbold, 2005b), in which this articular surface is considerably narrowed anteriorly between metatarsals 2 and 4. Later ornithomimids reduce the anterior aspect of metatarsal 3 to a greater extent, so that metatarsals 2 and 4 contact at their proximal ends (*Sinornithomimus*, LH PV7; Kobayashi and Lü, 2003). A previous reconstruction of the proximal articular end of metatarsal bundle of *Nqwebasaurus* erroneously attributed a portion of metatarsal 2 to metatarsal 3 (Choinere *et al.*, 2012: fig. 14C). In this way, metatarsal 3 appeared to be the largest proximal articular surface in the metatarsal bundle, a condition common among basal, non-tetanuran theropods.

The shaft of metatarsal 3 follows a gentle sigmoid curve in anterior view and is tightly appressed against nearly all but the distal extremities of the adjacent shafts of metatarsals 2 and 4 (Fig. 23.2). The distal one half of its shaft appears wedge-shaped, backed by the shafts of metatarsals 2 and 4. The shaft of metatarsal 4 is relatively slender along its entire length in *Nqwebasaurus*, measuring only one half the width of metatarsal 2 (Fig. 23.2, Tab. 4). The relatively slender shaft of metatarsal 4 compared to that of metatarsal 2 resembles the condition in *Ornitholestes* (Carpenter *et al.*, 2005) as apposed to the subequal shaft proportions of these two metatarsals in many other ornithomimosaurs (Osmólska *et al.*, 1972; Kobayashi and Barsbold, 2005b; Lee *et al.*, 2014). The lateral distal condyle of metatarsal 4 flares laterally to a greater degree than in *Harpymimus* (Kobayashi and Barsbold, 2005b) and many other ornithomimosaurs (Fig. 23.2).

Like other ornithomimosaurs, the non-ungual phalanges of pedal digit IV have stubby proportions, given the overall shortening of the phalangeal series. This also occurs in noasaurids (Carrano *et al.*, 2002) and alvarezsaurids (Novas,

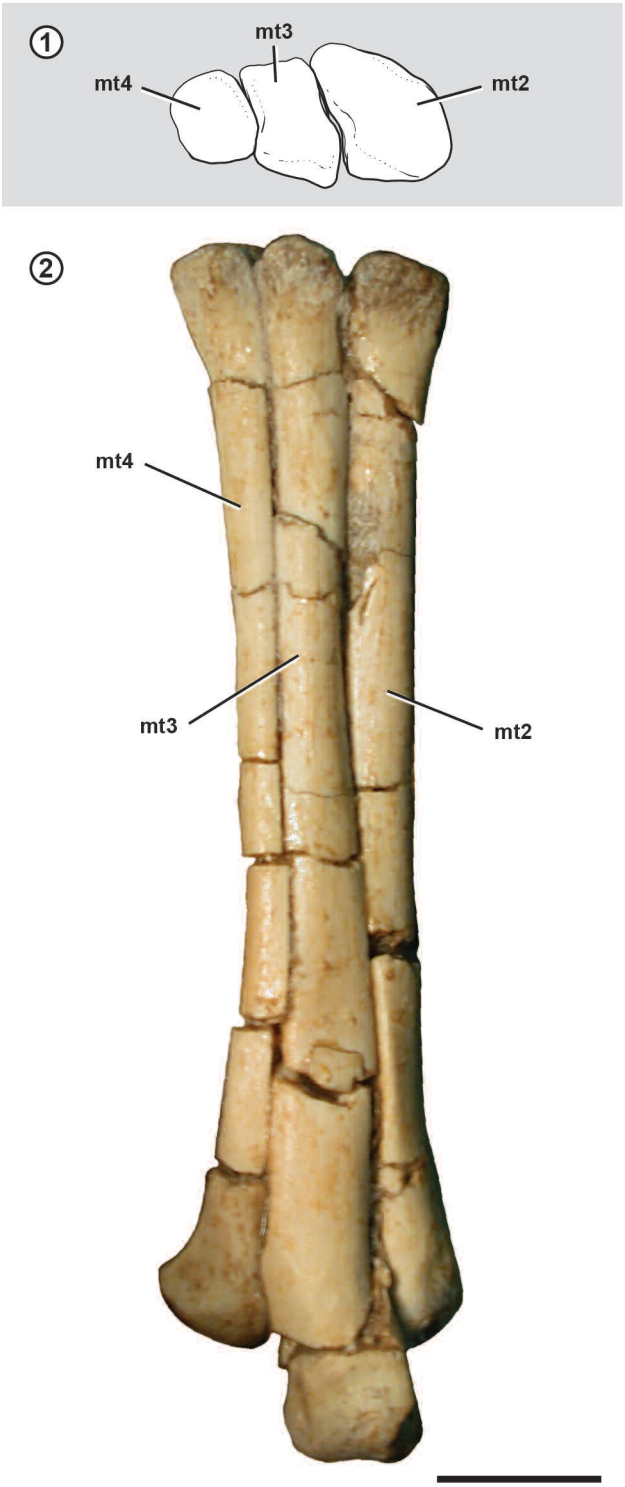

Figure 23. 1–2. ***Nqwebasaurus thwazi*, AM** 6040. Right metatarsals 2–4. **1,** proximal view (anterior toward bottom of page); **2,** anterior view. Abbreviations: **mt2-4,** metatarsal 2–4. Scale bar= 1 cm.

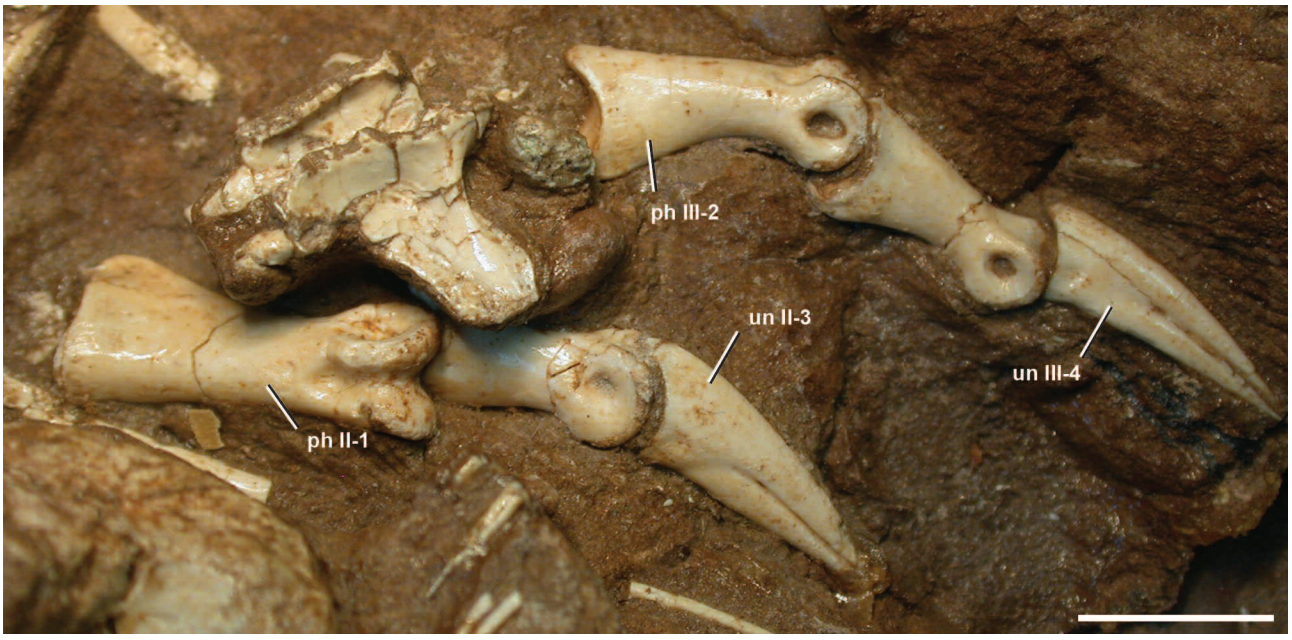

Figure 24. ***Nqwebasaurus thwazi*****, AM** 6040. Left pedal phalanges in dorsomedial view. Abbreviations: **II, III,** pedal digits II, III; **ph,** phalanx; **un,** ungual. Scale bar= 1 cm.

1997; Suzuki *et al.*, 2002). The pedal unguals are straight in lateral view, including the ungual of digit I (Figs. 22.1, 24). A raised, V-shaped platform and recessed flexor attachment depression are present ventrally in all pedal unguals (Choiniere *et al.*, 2012). In ornithomimosaurs, pedal ungual length varies. In *Gallimimus* the pedal unguals are short, with the unguals of digits III and IV subequal to their respective penultimate phalanges (Osmólska *et al.*, 1972). In *Sinornithomimus*, these same unguals are longer, approximately 125% of the length of their respective penultimate phalanges (LH PV7; Kobayashi and Lü, 2003). In *Nqwebasaurus*, these unguals are slight longer still, approximately 140% of the length of their respective penultimate phalanges (Figs. 22.2, 24).

DISCUSSION AND CONCLUSIONS

Nqwebasaurus*, basalmost ornithomimosaur.* This study adds to previous information (Choiniere *et al.*, 2012) supporting *Nqwebasaurus* as the basalmost ornithomimosaur. The skull appears to be considerably shorter-snouted than other ornithomimosaurs, based on the preserved length of the maxilla. *Nqwebasaurus* has a much narrower interorbital skull roof that lacks an enalrged prefrontal (Fig. 12.2). The preserved vertebrae, which include a series from the anteriormost dorsal through the mid cervicals, suggest that the skull was elevated well above the trunk in neutral pose.

The scapula and coracoid exhibit features that are distinctly primitive, such as the anteroventral, rather than everted, orientation of the scapular glenoid and the dorsal position on the corocid of the coracoid tubercle and subglenoid fossa (Fig. 16.3). The humerus has a broader deltopectoral crest and more primitive shaft curvature than in other ornithomimosaurs, and the manus is similarly primitve in the proportions of its metacarapals and phalanges and in the form of metacarpal-phalangeal and interphalageal joints (Fig. 18.3). The pubes appear to have a more abbreviate foot than in other ornithomimosaurs, and the pes retains a functioning, weight-bearing digit I and an unpinched proximal articular end to metatarsal 3 (Fig. 22). When formal phylogenetic consideration is given to the new information presented above, a considerable number of synapomorphies will solidify support for a clade of ornithomimosaurs exclusive of *Nqwebasaurus thwazi*, here termed Ornithomimoidea (Tab. 2).

Nqwebasaurus stands as the oldest known ornithomimosaur, discovered in a small outcrop of strata dated to the

earliest Cretaceous (Berriasian-Valanginian) approximately 140 Mya. Ornithomimosauria, nevertheless, must have diverged from other coleurosaurs at least some 25 My earlier, given the early Late Jurassic age of the oldest members of closely related clades, such as compsognathids (Dal Sasso and Maganuco, 2011) and alvarezsauroids (Choiniere *et al.*, 2010). Thus we are at an early stage in unraveling the early phylogenetic lines and biogeographic distribution of Ornithomimosauria.

Nqwebasaurus *and* Afromimus. Overlap between the preserved bones in the holotype of *Afromimus* and *Nqwebasaurus* is limited to aspects of the tibia, fibula, astragalus, and pedal unguals. The fibula shows the most striking differences. In *Afromimus*, the proximal end of the fibula is much more robust (Fig. 7). An elongate tibial crest extends distal to the cnemial crest and a prominent anterior trochanter is present on the proximal shaft. Neither are present in *Nqwebasaurus* (Fig. 21.1). The pedal ungual in *Afromimus* exhibits a dorsal, as well as a ventral, attachment groove (Fig. 10), whereas only the ventral groove is present in *Nqwebasaurus* (Fig. 24), *Sinornithomimus* (LH PV7) and other ornithomimosaurs.

A primitive feature present in *Afromimus*, the short length of the mid caudal prezygapophyses (Fig. 1), may indicate a basal position within Ornithomimosauria. The mid caudal prezygapophyses are more elongated in *Harpymimus* (Kobayashi and Barsbold, 2005b) and possibly also in *Shenzhousaurus* (Ji *et al.*, 2003). Two primitive features present in both *Afromimus* and *Nqwebasaurus* include the transversely expanded distal end of the fibula, which in the latter genus is based on the broad articular area for the distal end of the fibula on the tibia (Fig. 21.2). The ascending process of the astragalus also does not extend to the medial edge of the medial malleolus of the tibia in either genus (Figs. 6.1, 6.2; Choiniere *et al.*, 2012: fig. 13). The astragalus covers nearly all of the medial malleolus in western European ornithomimosaurs (Allain *et al.*, 2014), *Harpymimus*, (Kobayashi and Barsbold, 2005b), *Beishanlong* (Makovicky *et al.*, 2009), *Sinornithomimus* (LH PV7) and other Late Cretaceous ornithomimids (Osmólska *et al.*, 1972). In sum, there is very little information available at this time to effectively position *Afromimus* among basal ornithomimosaurs.

Afromimus*, basal ornithomimosaur.* Given the rarity of ornithomimosaurs on southern continents and previous records that have been reassigned to other therpod clades, is *Afromimus tenerensis* an ornithomimosaur? Some features of the tibia, fibula and ungual, in fact, have not been reported before among ornithomimosaurs, such as the raised medial buttress on the distal tibia (Fig. 6.1–2), the prominent anterior trochanter on the proximal fibula (Fig. 7), the partial coossification of tibia and fibula with the proximal tarsals (Figs. 6, 8), and the presence of an additional (dorsal) attachment groove on the pedal unguals (Fig. 10). These unusual features may indicate the presence of a fairly divergent taxon.

A few derived features are shared with other theropod clades, namely abelisauroids (abelisaurids, noasaurids). Relevant in this regard is the presence of an unnamed noasaurid in the fauna with *Afromimus* (Sereno *et al.*, 2004), to which direct comparison is possible.

Derived abelisauroid similarities include the V-shaped, ventral platform, weakened recurvature of the pedal unguals, and an additional (dorsal) attachment groove for the ungual sheath (Fig. 10). These features are present in pedal unguals of the noasaurid *Masiakasaurus* and in larger bodied abelisaurid unguals from South America and India (Carrano *et al.*, 2002; Novas and Bandyopadhyay, 2001), although in abelisauroid unguals the attachment grooves converge distally toward the tip of the ungual. In *Afromimus*, in contrast, the dorsal attachment groove dissipates before reaching the distal end of the ungual (Fig. 1). Finally, the dorsal attachment groove is absent altogether in the pedal unguals of the contemporaneous noasaurid from the El Rhaz Formation. Thus, abelisauroids consistently share only two features with *Afromimus* (ventral platform on weakly recurved pedal unguals), but these are also shared with Ornithomimosauria. *Masiakasaurus* also resembles *Afromimus* in the form of the distal fibula, which expands transversely and is partially fused to the ascending process (Fig. 8; Carrano *et al.*, 2002: fig. 16). The condition in the noasaurid from the El Rhaz Formation, however, is not as similar.

Many features present in the preserved material of *Afromimus* clearly distinguish it from the contemporary noasaurid, besides absence in the latter of a dorsal attachment groove on the pedal unguals. The tibial shaft of the noasaruid is straight and not bowed transversely as in *Afromimus* (Fig. 5). The proximal fibula is more slender and has a much weaker anterior troachanter than in *Afromimus*

(Fig. 7). The distal end of the fibula does not expand transversely, but rather is positioned along the anterolateral edge of the tibia, where it is coossified with the calcaneum. No caudal vertebrae are preserved for comparison.

The features favoring referral of *Afromimus* to the Ornithomisauria reside in the mid caudal vertebrae and pedal ungual. They include, first, the very broad peanut-shaped articular faces of mid caudal vertebrae and, second, parasagittal fossa that receive the postzygapophyseal processes of the preceding mid caudal vertebra (Fig. 1). The former appears to stabilize the tail from lateral flexion, whereas the latter appears to stiffen the tail in a manner similar to hypertrophied prezygapophyseal processes among paravians. These features are present in *Sinornithomimus* (LH PV7), *Gallimimus* (Osmólska *et al.*, 1972) and other Late Cretaceous ornithomimosaurs (Longrich, 2008). Caudal centra with very broad articular faces are present in the stout-limbed *Deinocheirus* (Lee *et al.*, 2014).

Although previously unrecognized as ornithomimosaurian synapomorphies, these derived features of the mid caudal vertebrae have not been reported outside Ornithomimosauria. Abelisauroid mid caudal centra have subcircular articular faces (*Majungasaurus*; O'Connor, 2007) or faces that are slightly broader than deep (*Masiakasaurus*; Carranno *et al.*, 2002). Alvarezsaurids (Novas, 1997; Suzuki *et al.*, 2002) and short-tailed coelurosaurian theropods, such as some therizinosaurids (Zanno, 2010) and oviraptorids (Barsbold *et al.*, 2000), do not exhibit broad caudal centra with interlocking zygapophyses. The pedal ungual of *Afromimus* (Fig. 10), as noted above, resembles ornithomimosaurs most notably by the straight ventral margins of the ungual, V-shaped ventral platform, and recessed flexor attachment pit, features that are at least partially reversed in the stout-limbed *Beishanlong* (Makovicky *et al.*, 2009) and *Deinocheirus* (Lee *et al.*, 2014). The affinities of *Afromimus* will likely be tested most effectively by discovery of new material from the El Rhaz Formation or overlapping finds from other localities.

ACKNOWLEDGMENTS

I would like to thank C. Abraczinskas for the pencil drawings, L. Conroy for line drawings, labeling and layout, W. J. de Klerk for access to specimens in his care, Federico Agnolín and Ronan Allain for their constructive reviews, my field teams for fortitude under trying conditions, and the République du Niger for permission to conduct field work.

REFERENCES

Allain, R., Vullo, R., Le Loeuff, J., and Tournepiche, J.-F. 2014. European ornithomimosaurs (Dinosauria, Theropoda): an undetected record. *Geologica Acta* 12: 127–135.

Alifanov, V.R., and Saveliev, S.V. 2015. The most ancient ornithomimosaur (Theropoda, Dinosauria), with cover imprints from the Upper Jurassic of Russia. *Paleontological Journal* 49: 636–650.

Angolin, F.L., Ezcurra, M.D., Pais, D.F., and Salisbury, S.W. 2010. A reappraisal of the Cretaceous non-avian dinosaur faunas from Australia and New Zealand: evidence for their Gondwanan affinities. *Journal of Systematic Palaeontology* 8: 257–300.

Barsbold, R. 1976. On the evolution and systematics of the late Mesozoic dinosaurs. *Paleontologiâ i biostratigrafiâ Mongolii. Sovmestnaâ Sovetsko-Mongolskaâ Paleontologičeskaâ Ekspediciâ, Trudy* 3: 68–75. [in Russian.].

Barsbold, R. 1981. Toothless carnivorous dinosaurs of Mongolia. *Trudy Sovmestnoi Sovetsko-Mongol'skoi Paleontologicheskoi Ekspeditsii* 15: 28–39.

Barsbold, R., and Perle, A. 1984. 1st finding of primitive ornithomimosauria from the Cretaceous period of the MPR (Mongolian Peoples-Republic). *Paleontologicheskii Zhurnal*: 121–123.

Barsbold, R., Osmólska, H., Watabe, M., Currie, P.J., and Tssogtbaatar, K. 2000. A new oviraptorosaurs (Dinosauria: Theropoda) from Mongolia: The first dinosaur with a pygostyle. *Acta Palaeontologia Polonica* 45: 97–106.

Brochu, C.A. 2003. Osteology of *Tyrannosaurus rex*: Insights from a nearly complete skeleton and high-resolution computed tomographic analysis of the skull. *Journal of Vertebrate Paleontology*, *Memoir 7* 22: 1–138.

Brownstein, C.D. 2017. Description of Arundel Clay ornithomimosaur material and a reinterpretation of *Nedcolbertia justinhofmanni* as an "Ostrich Dinosaur": biogeographic implications. *PeerJ* 5: e3110.

Brusatte, S.L., Benson, R.B.J., and Hutt, S. 2008. The osteology of Neovenator salerii (Dinosauria: Theropoda) from the Wealden Group (Barremian) of the Isle of Wight. Monograph of the Palaeontographical Society 2008: 1–75.

Buffetaut, E., Suteethorn, V., and Tong, H. 2009. An early "ostrich dinosaur" (Theropoda: Ornithomimosauria) from the Early Cretaceous Sao Khua Formation of NE Thailand. *Geological Society, London, Special Publications* 315: 229–243.

Carpenter, K., Miles, C., Ostrom, J.H., and Cloward, K. 2005. Redescription of the small maniraptoran theropods *Ornitholestes* and *Coelurus* from the Upper Jurassic Morrison Formation of Wyoming. In: K. Carpenter (Ed.), *The Carnivorous Dinosaurs*, Indiana University Press, Bloomington, p. 49–71.

Carrano, M.T., Sampson, S.D., and Forster, C.A. 2002. The osteology of *Masiakasaurus knopfleri*, a small abelisauroid (Dinosauria: Theropoda) from the Late Cretaceous of Madagascar. *Journal of Vertebrate Paleontology* 22: 510–534.

Carrano, M.T. and Hutchinson, J.R. 2002. Pelvic and hindlimb musculature of *Tyrannosaurus rex* (Dinosauria: Theropoda). *Journal of Morphology* 253: 207–228.

Carrano, M.T., Loewen, M.A., and Sertich, J.J. 2011. New materials of *Masiakasaurus knopfleri* Sampson, Carrano, and Forster, 2001, and implications for the morphology of the Noasauridae (Theropoda: Ceratosauria). *Smithsonian Contributions to Paleobiology* 95: 1–53.

Chiappe, L.M., Norell, M.A., and Clark, J.M. 1998. The skull of a relative of the stem-group bird *Mononykus*. *Nature* 392: 275–278.

Choiniere, J.N., Xu, X., Clark, J.M., Forster, C.A., Guo, Y., and Han, F. 2010. A basal alvarezsauroid theropod from the early Late

Jurassic of Xinjiang, China. *Science* 327: 571–574.

Choiniere, J.N., Forster, C.A., and de Klerk, W.J. 2012. New information on *Nqwebasaurus thwazi*, a coelurosaurian theropod from the Early Cretaceous Kirkwood Formation in South Africa. *Journal of African Earth Sciences* 71: 1–17.

Currie, P.J. and Zhao, X-J. 1993. A new carnosaur (Dinosauria: Theropoda) from the Jurassic of Xinjiang, People's Republic of China. *Canadian Journal of Earth Sciences* 30: 2037–2081.

Dal Sasso, C., and Maganuco, S. 2011. *Scipionyx samniticus* (Theropoda: Compsognathidae) from the Lower Cretaceous of Italy. *Memorie della Societa italiana di scienze naturali e del Museo civico di storia naturale di Milano* 37: 1–281.

de Klerk, W.J., Forster, C.A., Sampson, S.D., Chinsamy, A., and Ross, C.F. 2000. A new coelurosaurian dinosaur from the Early Cretaceous of South Africa. *Journal of Vertebrate Paleontology* 20: 324–332.

Galton, P.M. 1982. *Elaphrosaurus*, an ornithomimid dinosaur from the Upper Jurassic of North America and Africa. *Paläontologische Zeitschrift* 56: 265–275.

Galton, P.M., and Molnar, R.E. 2005. Tibiae of small theropod dinosaurs from southern England: from the Middle Jurassic of Stonesfield near Oxford and the Lower Cretaceous of the Isle of Wight. In: K. Carpenter (Ed.), *The Carnivorous Dinosaurs*, Indiana University Press, Bloomington, p. 3–22.

Holtz, T.R. 1994. The phylogenetic position of the Tyrannosauridae: implications for theropod systematics. *Journal of Paleontology* 68: 1100–1117.

Huene, F. von. 1914. Das natürliche system der Saurischia. *Zentralblatt Mineralogie, Geologie, und Palaeontologie B*: 154–158.

Ji, Q., Norell, M.A., Makovicky, P.J., Gao, K.Q., Ji, S.A., and Yuan, C. 2003. An early ostrich dinosaur and implications for ornithomimosaur phylogeny. *American Museum Novitates* 3420: 1–19.

Jin, L., Chen, J., and Godefroit, P. 2012. A new basal ornithomimosaur (Dinosauria: Theropoda) from the early Cretaceous Yixian formation, northeast China. In: P. Godefroit (Ed.), *Bernissart Dinosaurs and Early Cretaceous Terrestrial Ecosystems*, Indiana University Press, Bloomington, p. 467–487.

Kirkland, J.I., Britt, B.B., Whittle, C.H., Madsen, S.K., and Burge, D.L. 1998. A small coelurosaurian theropod from the Yellow Cat Member of the Cedar Mountain Formation (Lower Cretaceous, Barremian) of eastern Utah. In: S.G. Lucas, J.I. Kirkland, and J.W. Estep, (Eds.), *Lower and Middle Cretaceous Ecosystems*. New Mexico Museum of Natural History and Science Bulletin 14, New Mexico, pp. 239–248.

Kobayashi, Y., and Barsbold, R. 2005a. Reexamination of a primitive ornithomimosaur, *Garudimimus brevipes* Barsbold, 1981 (Dinosauria: Theropoda), from the Late Cretaceous of Mongolia. *Canadian Journal of Earth Sciences* 42: 1501–1521.

Kobayashi, Y., and Barsbold, R. 2005b. Anatomy of *Harpymimus okladnikovi* Barsbold and Perle 1984 (Dinosauria; Theropoda) of Mongolia. In: K. Carpenter (Ed.), *The Carnivorous Dinosaurs*, Indiana University Press, Bloomington, p. 97–126.

Kobayashi, Y., and Lü, J.C. 2003. A new ornithomimid dinosaur with gregarious habits from the Late Cretaceous of China. *Acta Palaeontologica Polonica* 4: 235–259.

Lee, Y.N., Barsbold, R., Currie, P.J., Kobayashi, Y., Lee, H.J., Godefroit, P., Escuillié, F., and Chinzorig, T. 2014. Resolving the long-standing enigmas of a giant ornithomimosaur *Deinocheirus mirificus*. *Nature* 515: 257–260.

Leidy, J. 1856. Notice of remains of extinct reptiles and fishes, discovered by Dr. F. V. Hayden in the badlands of the Judith River, Nebraska Territory. *Proceedings of the Academy of Natural Sciences of Philadelphia* 8: 72–73.

Linnaeus, C. 1758. *Systema Naturae per Raegna Tria Naturae. Volume 1. Regnum Animale.* 10th [photographic facsimile] edition, Trustees, British Museum (Natural History), London, 823 p.

Longrich, N. 2008. A new, large ornithomimid from the Cretaceous Dinosaur Park Formation of Alberta, Canada: implications for the study of dissociated dinosaur remains. *Palaeontology* 51: 983–997.

Makovicky, P.J., Li, D., Gao, K.Q., Lewin, M., Erickson, G.M., and Norell, M.A. 2009. A giant ornithomimosaur from the Early Cretaceous of China. *Proceedings of the Royal Society of London B: Biological Sciences* 277: 191–198.

Maleev, E.A. 1954. New turtle-like reptile in Mongolia. *Priroda* 3: 106–108.

Marsh, O.C. 1890. Description of new dinosaurian reptiles. *American Journal of Science*: 81–86.

Marsh, O.C. 1891. The Gigantic Ceratopsidae, or Horned Dinosaurs, of North America. *Geological Magazine* 8: 193–199.

Martinez, R.N., Sereno, P.C., Alcober, O.A., Colombi, C.E., Renne, P.R., Montañez, I.P., and Currie, B.S. 2011. A basal dinosaur from the dawn of the dinosaur era in southwestern Pangaea. *Science* 331: 306–210.

Nicholls, E.L., and Russell, A.P. 1985. Structure and function of the pectoral girdle and forelimb of *Struthiomimus altus* (Theropoda: Ornithomimidae). *Palaeontology* 28: 643–677.

Novas, F.E. 1997. Anatomy of *Patagonykus puertai* (Theropoda, Avialae, Alvarezsauridae), from the Late Cretaceous of Patagonia. *Journal of Vertebrate Paleontology* 17: 137–166.

Novas, F.E., and Bandyopadhyay, S. 2001. Abelisaurid pedal unguals from the Late Cretaceous of India. *VII International Symposium on Mesozoic Terrestrial Ecosystems* (Buenos Aires) Publicación Electrónica de la Asociación Paleontológica Argentina, Special Publication 7: 145–149.

O'Connor, P.M. 2007. The postcranial axial skeleton of *Majungasaurus crenatissimus* (Theropoda: Abelisauridae) from the Late Cretaceous of Madagascar. *Journal of Vertebrate Paleontology, Memoir 8, supplement 2* 27: 127–162.

Osborn, H.F. 1905. *Tyrannosaurus* and other Cretaceous carnivorous dinosaurs. *Bulletin of the American Museum of Natural History* 21: 259–265.

Osborn, H.F. 1917. Skeletal adaptations of *Ornitholestes, Struthiomimus, Tyrannosaurus. Bulletin of the American Museum of Natural History* 35: 733–771.

Osborn, H.F. 1924. Sauropoda and Theropoda of the Lower Cretaceous of Mongolia. *American Museum Novitates* 128: 1–7.

Osmólska, H., and Roniewicz, E. 1970. Deinocheiridae, a new family of theropod dinosaurs. *Acta Palaeontologica Polonica* 21: 5–19.

Osmólska, H., Roniewicz, E., and Barsbold, R. 1972. A new dinosaur, *Gallimimus bullatus* n. gen., n. sp. (Ornithomimidae) from the Upper Cretaceous of Mongolia. *Acta Palaeontologica Polonica* 27: 103–143.

Ostrom, J.H. 1978. The osteology of *Compsognathus longipes* Wagner. *Zitteliana* 4: 73–118.

Owen, R. 1842. Report on British fossil reptiles, part II. *Report of the British Association for the Advancement of Science* 11: 60–204.

Pérez-Moreno, B.P., Sanz, J.L., Buscalioni, A.D., Moratalla, J.J., Ortega, F., and Rasskin-Gutman, D. 1994. A unique multitoothed ornithomimosaur dinosaur from the Lower Cretaceous of Spain. *Nature* 370: 363–367.

Rauhut, O.W., and Carrano, M.T. 2016. The theropod dinosaur *Elaphrosaurus bambergi* Janensch, 1920, from the Late Jurassic of Tendaguru, Tanzania. *Zoological Journal of the Linnean Society*

178: 546–610.

Rich, T.H., and Rich, P.V. 1994. Neoceratopsians and ornithomimosaurs: Dinosaurs of Gondwana origin? *National Geographic Research & Exploration* 10: 132–134.

Seeley, H.G. 1888. Classification of the Dinosauria. *Geological Magazine* 5: 45–46.

Sereno, P.C. 1994. The pectoral girdle and forelimb of the basal theropod *Herrerasaurus ischigualastensis*. *Journal of Vertebrate Paleontology* 13: 425–450.

Sereno, P.C. 1999a. The evolution of dinosaurs. *Science* 284: 2137–2147.

Sereno, P.C. 1999b. A rationale for dinosaurian taxonomy. *Journal of Vertebrate Paleontology* 19: 788–790.

Sereno, P.C. 2001. Alvarezsaurids: birds or ornithomimosaurs? In: J. Gauthier, and L.F. Gall (Eds.), *New Perspectives on the Origin and Early Evolution of Birds*, Yale University, New Haven, p. 69–98.

Sereno, P.C. 2005a. TaxonSearch: a relational database for suprageneric taxa and phylogenetic definitions. *PhyloInformatics* 8: 1–21.

Sereno, P.C. 2005b. Stem Archosauria—*TaxonSearch*. *URL* http://www.taxonsearch.org/dev/file_home.php [version 1.0 2005 Nov 7].

Sereno, P.C., Dutheil, D.B., Iarochene, M., Larsson, H.C.E., Lyon, G.H., Magwene, P.M., Sidor, C.A., Varricchio, D.J., and Wilson, J.A. 1996. Predatory dinosaurs from the Sahara and Late Cretaceous faunal differentiation. *Science* 272: 986–991.

Sereno, P.C., Martinéz, R.N., and Alcober, O.A. 2012. Osteology of *Eoraptor lunensis* (Dinosauria: Sauropodomorpha). *Journal of Vertebrate Paleontology, Memoir 12, supplement 1* 32: 81–177.

Sereno, P.C., Wilson, J.A., and Conrad, J.L. 2004. New dinosaurs link southern landmasses in the Mid–Cretaceous. *Proceedings of the Royal Society of London B* 271: 1325–1330.

Shapiro, M.D., You, H., Shubin, N.H., Luo, Z., and Downs, J.P. 2003. A large ornithomimid pes from the Lower Cretaceous of the Mazongshan area, northern Gansu Province, People's Republic of China. *Journal of Vertebrate Paleontology* 23: 695–698.

Sternberg, C.M. 1933. A new *Ornithomimus* with complete abdominal cuirass. *Canadian Field Naturalist* 47: 79–83.

Suzuki, S., Chiappe, L.M., Dyke, G.J., Watanabe, M., Barsbold, R., and Tsogtbaatar, K. 2002. A new specimen of *Shuvuuia deserti* Chiappe *et al.*, 1998 from the Mongolian Late Cretaceous with a discussion of the relationships of alvarezsaurids to other theropod dinosaurs. *Natural History Museum of Los Angeles County, Contributions in Science* 494: 1–18.

Varricchio, D.J., Sereno, P.C., Zhao, X., Tan, L., Wilson, J.A., and Lyon, G.H. 2008. Mud-trapped herd captures evidence of distinctive dinosaur sociality. *Acta Palaeontologica Polonica* 53: 567–578.

Wilson, J.A. 1999. A nomenclature for vertebral laminae in sauropods and other saurischian dinosaurs. *Journal of Vertebrate Paleontology* 19: 639–653.

Wilson, J.A. 2006. Anatomical nomenclature of fossil vertebrates: standardized terms or 'lingua franca'? *Journal of Vertebrate Paleontology* 26: 511–518.

Wilson, J.A., Michael, D.D., Ikejiri, T., Moacdieh, E.M., and Whitlock, J.A. 2011. A nomenclature for vertebral fossae in sauropods and other saurischian dinosaurs. *PLoS ONE* 6: e17114.

Zanno, L.E. 2010. Osteology of *Falcarius utahensis* (Dinosauria: Theropoda): characterizing the anatomy of basal therizinosaurs. *Zoological Journal of the Linnean Society* 158: 196–230.

doi: 10.5710/AMGH.23.10.2017.3155

Submitted: August 5th, 2017
Accepted: October 23rd, 2017
Published online: November 1st, 2017